Metrology and Dosimetry of At-211 Radiolabeled Compounds

Gamal Akabani, Ph.D.

TRT Dosimetry Workshop
April 19-20, 2018

Outline

- Physical and radiobiological characteristics of At-211
- Production methods and sites
- In Vitro Studies
- Preclinical Studies
- Clinical Trials
- Conclusions

Physical Characteristics of At-211

- Astatine was produced for the first time at the University of California in 1940 by Dale R. Corson, K.R. Mackenzie, and Emilio Segré.
- Half-life: 7.214 h
- Classical production:
  - $^{209}Bi(\alpha,2n)^{211}At$ - 28 MeV using a mid energy cyclotron
  - $^{211}Rn/^{211}At$ generator system - TRIUMF's Isotope Separator and Accelerator (ISAC) facility – Very complex procedure
- There was no suitable surrogate for molecular imaging until At-209 was produced at TRIUMF

Physical Characteristics of Several Radioisotopes Used for Targeted Radionuclide Therapy

Isotope	Half-life (h)	Particle Emitted for Therapy	Maximum Energy (keV)	Maximum Range in Tissue (mm)
Iodine-131 (^{131}I)	193	β	970	2.0
Rhenium-186 (^{186}Re)	91	β	1,080	11.0
Rhenium-188 (^{188}Re)	17	β	2,120	11.0
Yttrium-90 (^{90}Y)	64	β	2,280	1.2
Lutetium-177 (^{177}Lu)	161	β	496	1.5
Copper-67 (^{67}Cu)	62	β	577	1.8
Bismuth-213 (^{213}Bi)	0.76	α	8,376	0.08
Bismuth-212 (^{212}Bi)	1	α	8,780	0.09
Actinium-225 (^{225}Ac)	240	α	>6,000	0.08
Astatine-211 (^{211}At)	7.2	α	7,450	0.07
Radium-223 (^{223}Ra)	274.32	α+	>5,000	0.08
Thorium-227 (^{227}Th)	448.32	α+	>6,000	0.08

The half-life of the selected radionuclide must correspond with the biological half-life of the monoclonal antibody for maximum delivery

The Decay Scheme of At-211

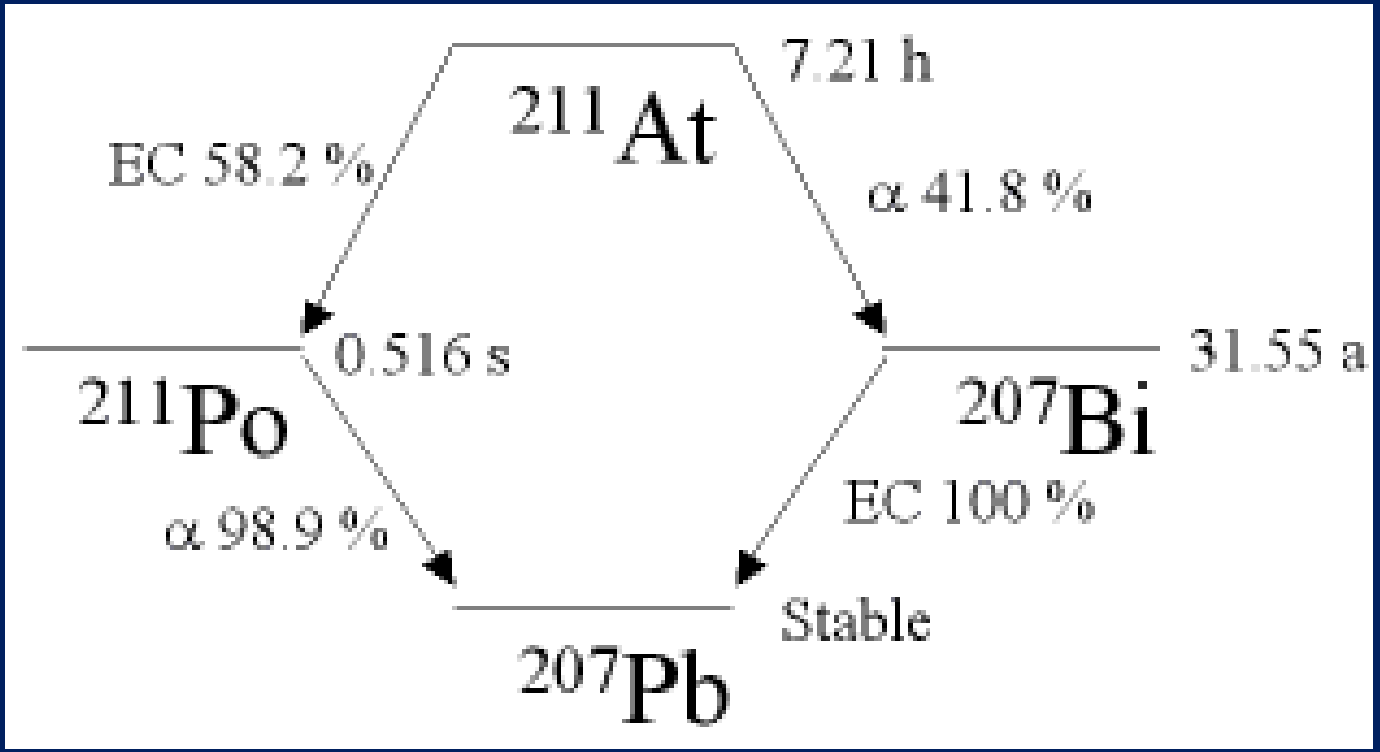

At-211

Alpha Particle Energy (MeV)	Intensity (%)	Range in Tissue (μm)	# of Cell Diameters
5.87	41.94	47.98	3.2
6.57	0.337	57.26	3.8
6.89	0.325	61.78	4.1
7.45	57.4	69.92	4.7

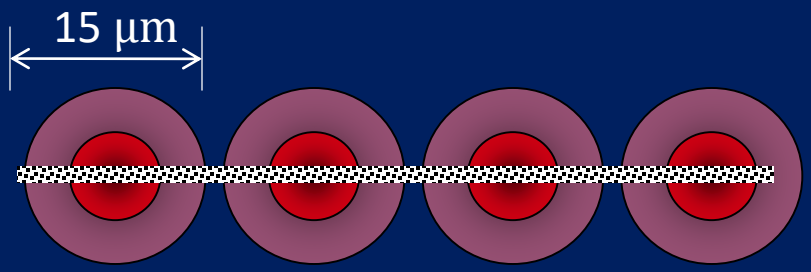

Only two or three alpha particle hits to the nucleus are required to sterilize a tumor cell

Production centers

- Europe : 21 centers
- Americas: 8 centers
- Asia: 7 centers

M. R. Zalutsky and M. Pruszynski, “Astatine-211: production and availability.,” *Current radiopharmaceuticals*, vol. 4, no. 3, pp. 177–185, Jul. 2011.

Micrometastases: Early Dissemination

- Although primary tumors are diagnosed at a still earlier stage, many patients will have circulating tumor cells and sub-clinical micro-metastases in other organs at the time when the primary tumor is surgically removed.

Braun S, Vogl FD, Naume B et al (2005) A pooled analysis of bone marrow micrometastasis in breast cancer. N Engl J Med 353:793–802.

Alix-Panabières C, Müller V, Pantel K. (2007) Current status in human breast cancer micrometastasis. Curr Opin Oncol. 19:558-63.

Therapeutic Strategies

- Must Take into account the ***spatiotemporal phatophysiology*** of
  - Tumor growth, Invasion, Migration, Circulating Tumor Cells, and Micro-metastases based on tumor cell heterogeneity and micro-environmental conditions.
- Develop potential combinatorial strategies
  - Anti-tumoral
  - Anti-invasive
  - Anti-angiogenic
  - Anti-vascular
  - Anti-metastatic, eradication of circulating tumor cells (CTC) and circulating cancer steam cells (CSC) and micro-metastatic disease
- Different 'targets' require careful selection of a biological (mAb) and radionuclide

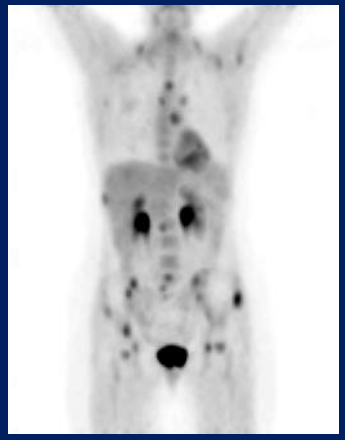

In Vitro Studies

Key Factors in TRT

- Pharmacokinetics and Pharmacodynamics (PB and MB PK/PD)
  - Organ distribution, morphological distribution, diffusion, association rate, k_a, *d*issociation rate, k_d , *i*nternalization rate, k_e, expulsion rate, k_x
- Tumor morphology, spatiotemporal pathophysiology, and micro-environmental factors
- Radiochemistry:
  - Selection, chemistry, labeling, and *in vivo* stability
  - ***Radiative emissions (α, ß) and range in tissue***

The role of MB PK/PD in TRT

Describe

Predict

Understand

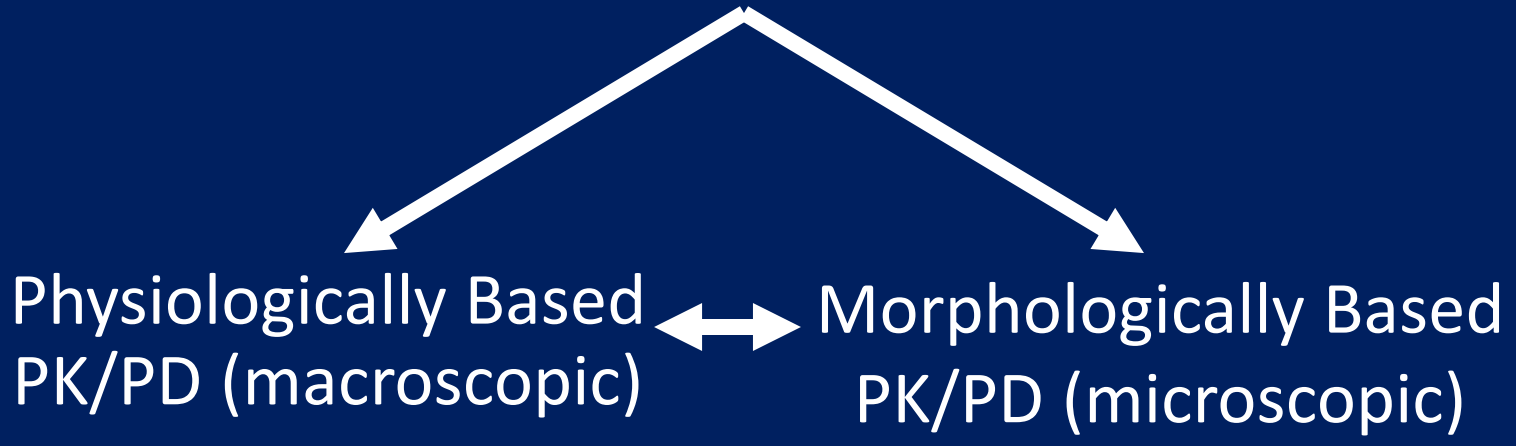

PB PK/PD Models

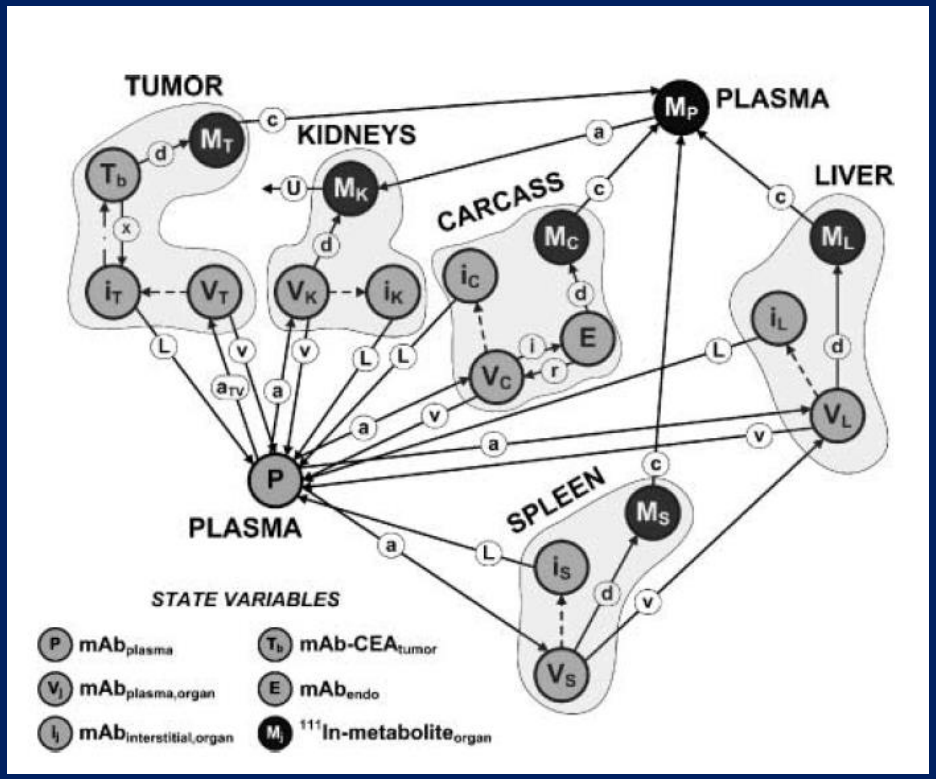

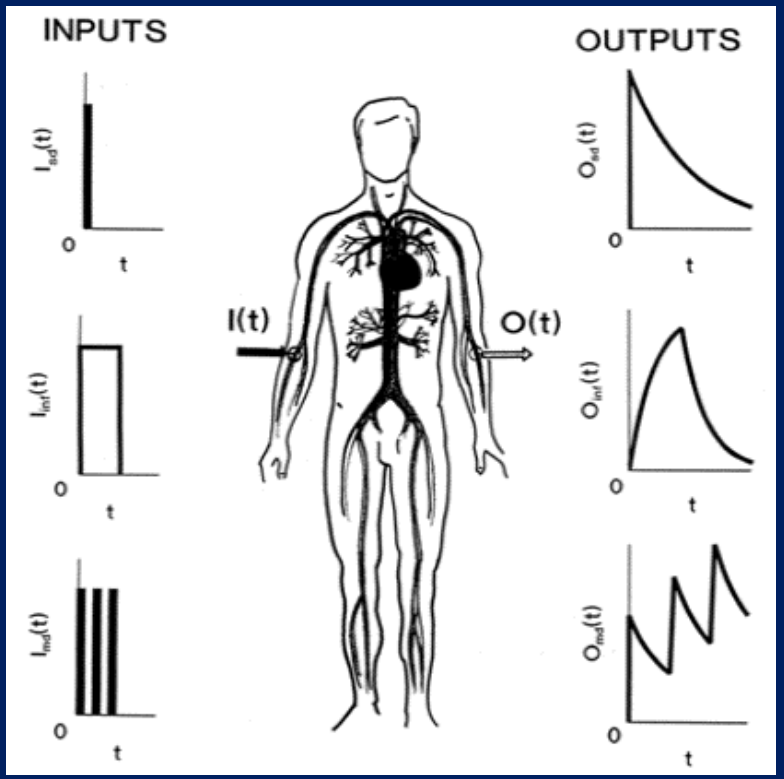

Limitations and Obstacles on Diffusion of Radiolabeled Compounds

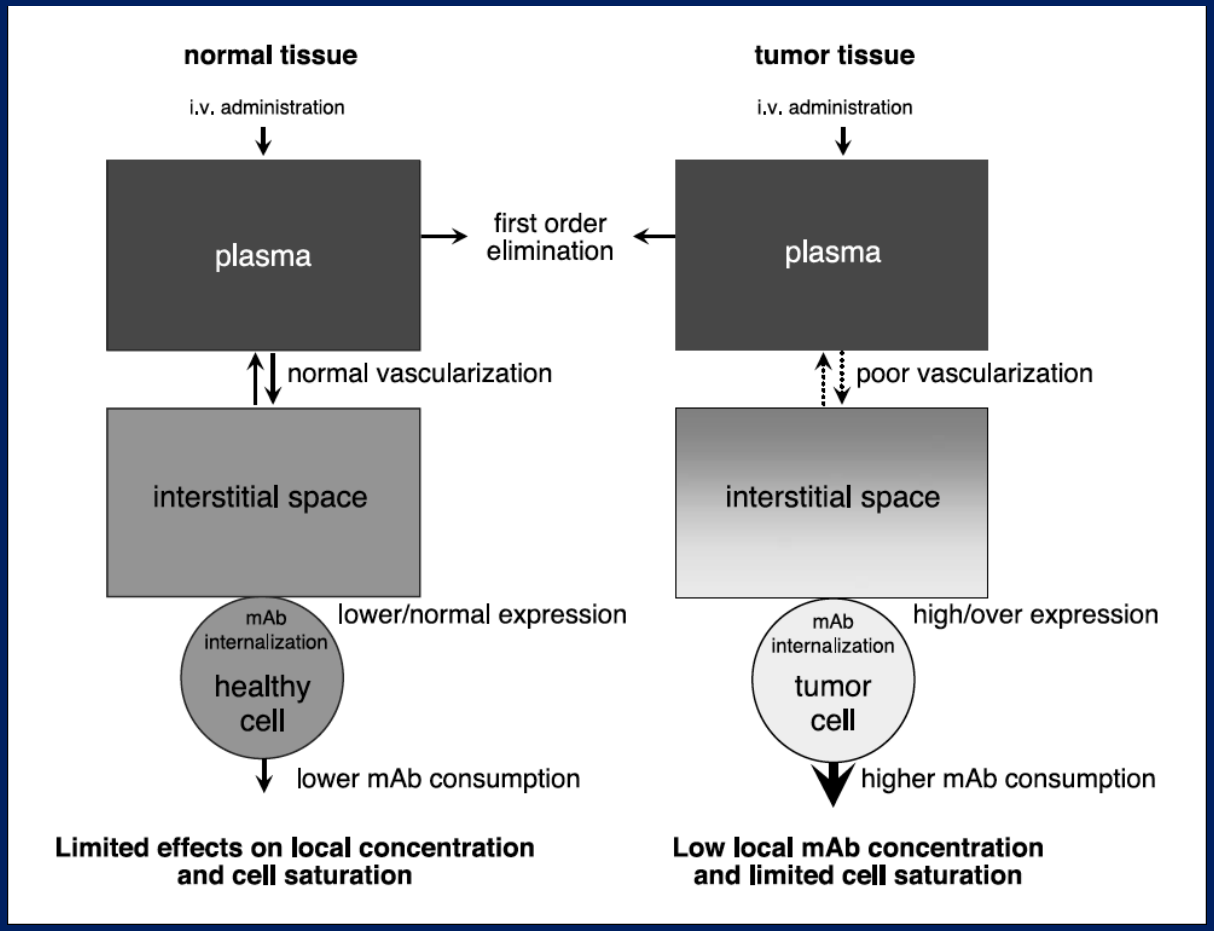

Morphologically Based PK/PD

- Competitive processes between labeled (hot) and unlabeled (cold) monoclonal antibodies

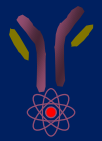

Labeled (hot)

Unlabeled (cold)

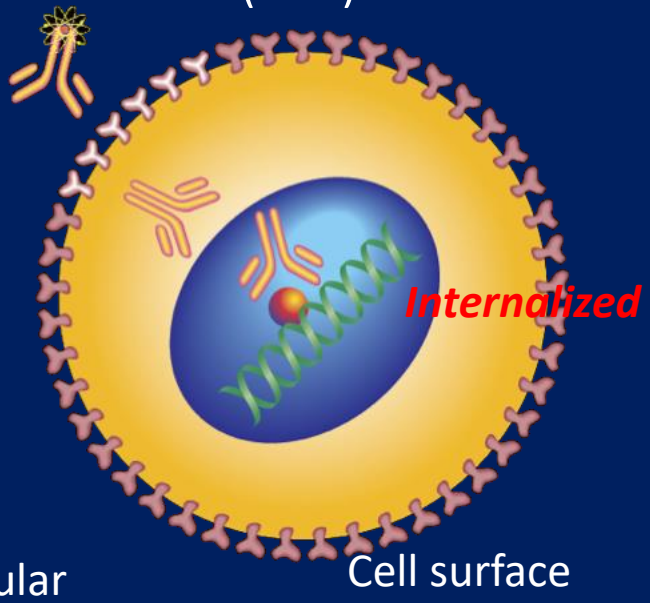

- Morphological barriers, micro-distribution
- Sources of radiation
  - Medium (Extra-cellular space)
  - Cell Surface
  - Internalized

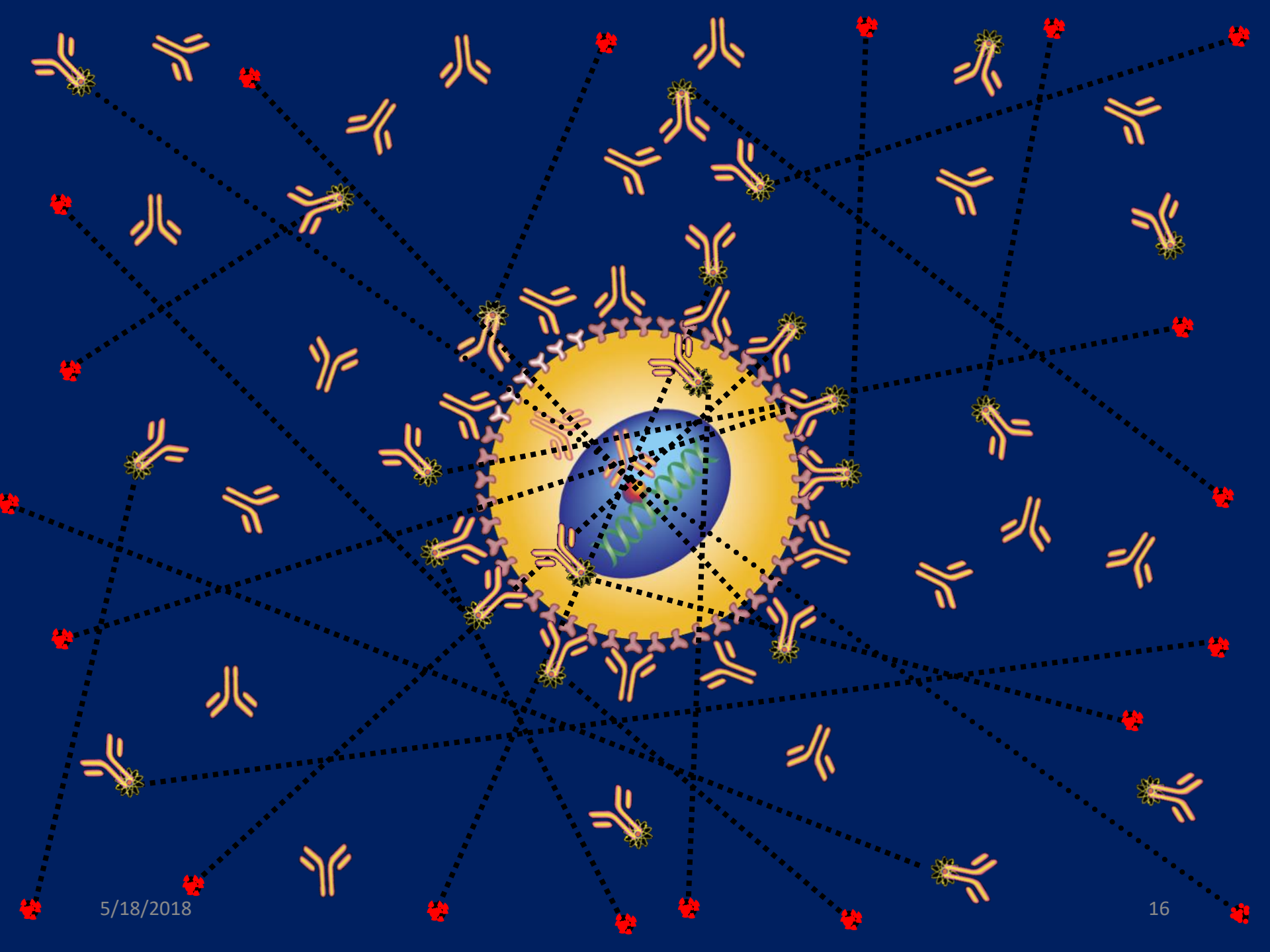

Alpha Particle Monte Carlo Transport – Single Event

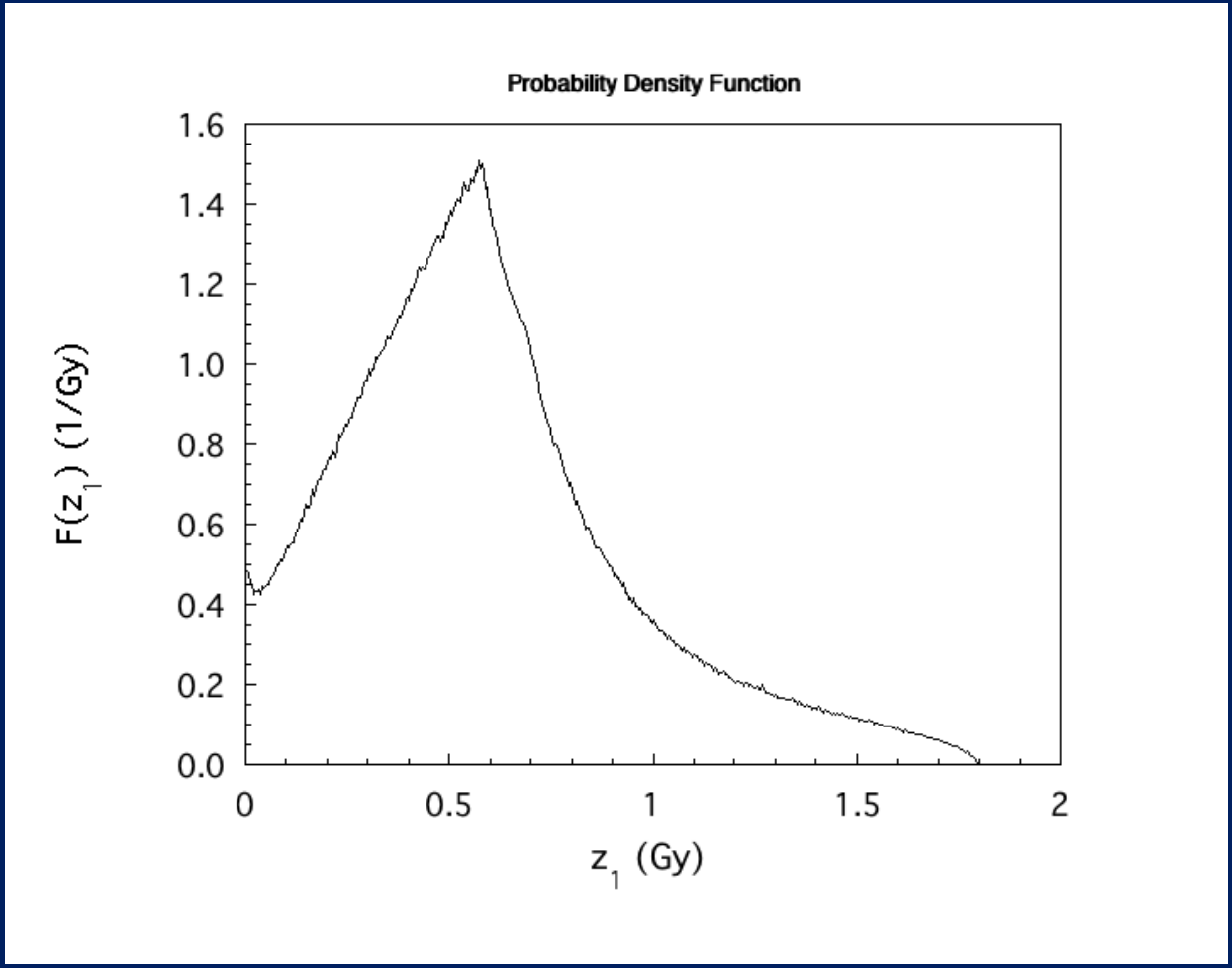

Alpha Particle Monte Carlo Transport – Point Kernel

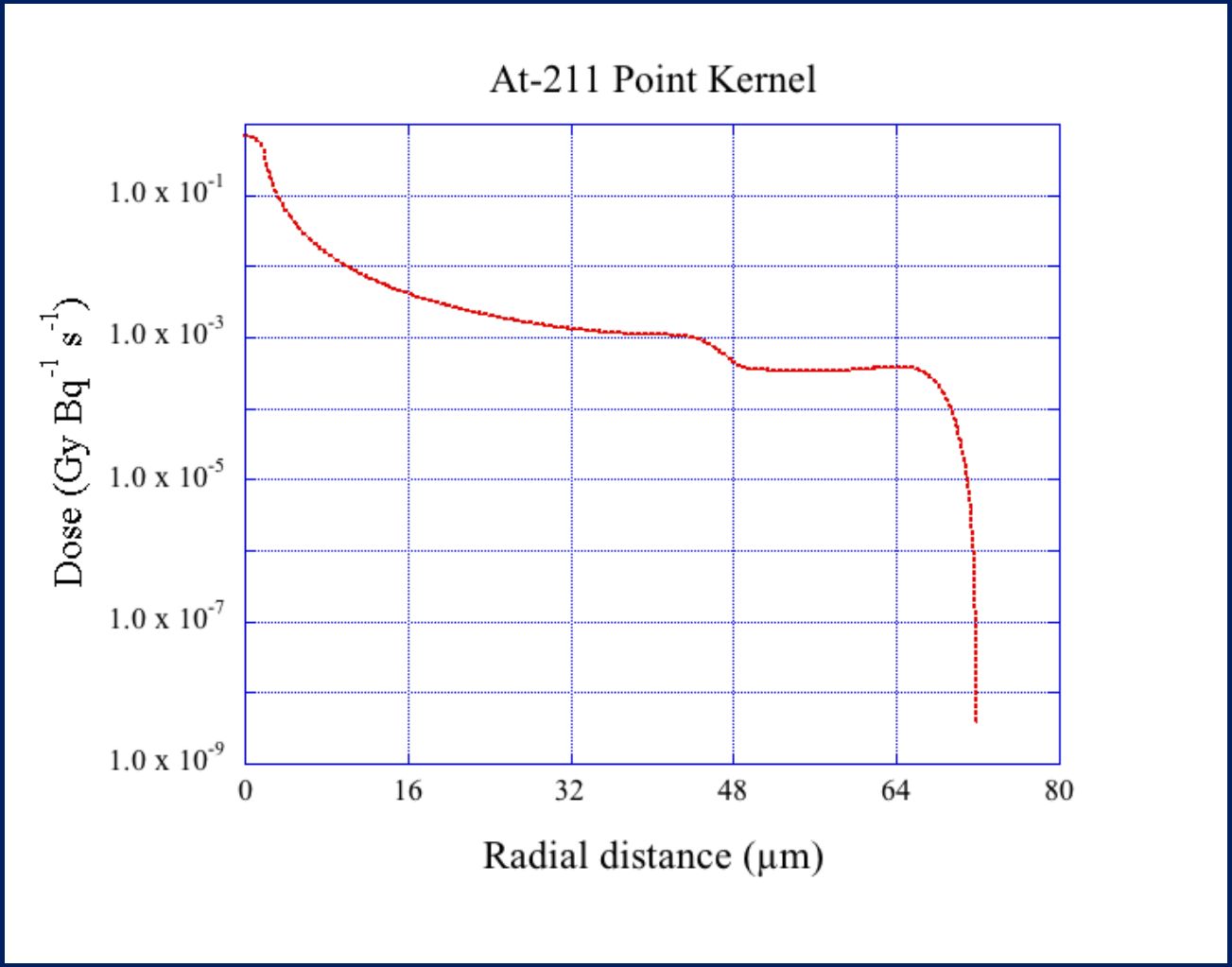

Average Maximum Binding Capacity, B_{max}

B_{max}: average number of receptors per cell

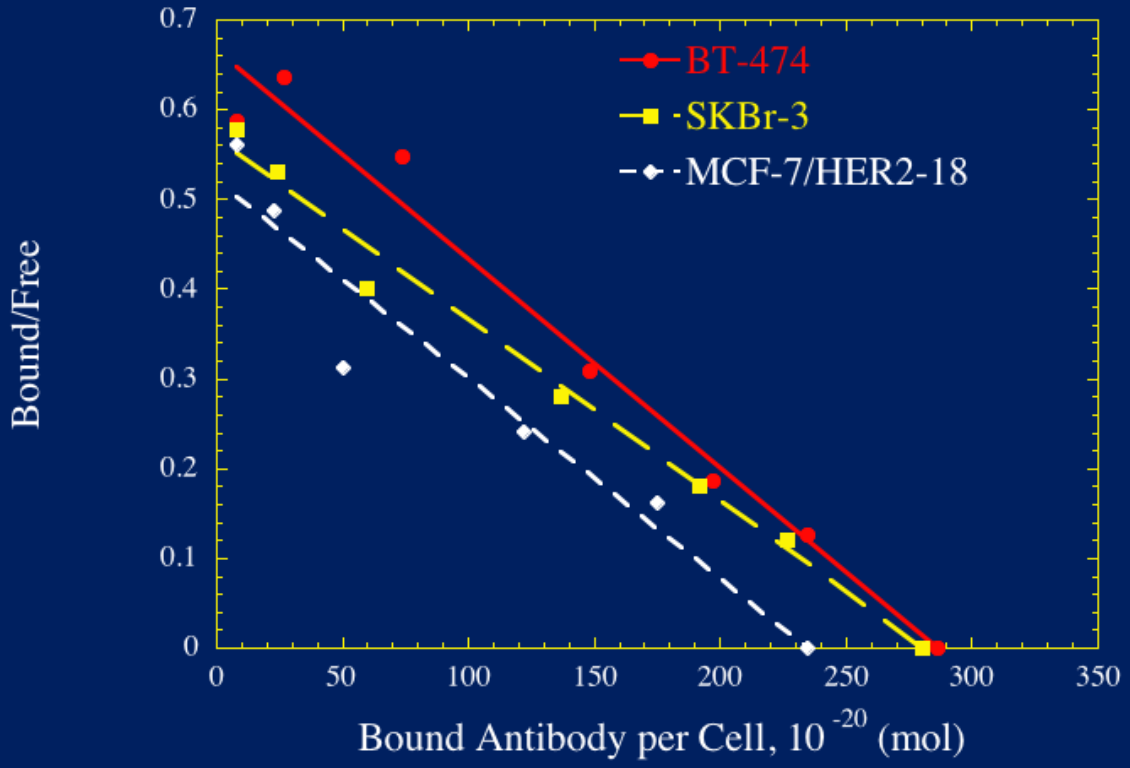

	BT-474	SKBr-3	MCF-7/HER2-18
B_{max}	1.72×10^6	1.69×10^6	1.41×10^6

Relative HER2 Receptor Expression:
Fluorescent-Activated Cell Sorting (FACS) Analysis

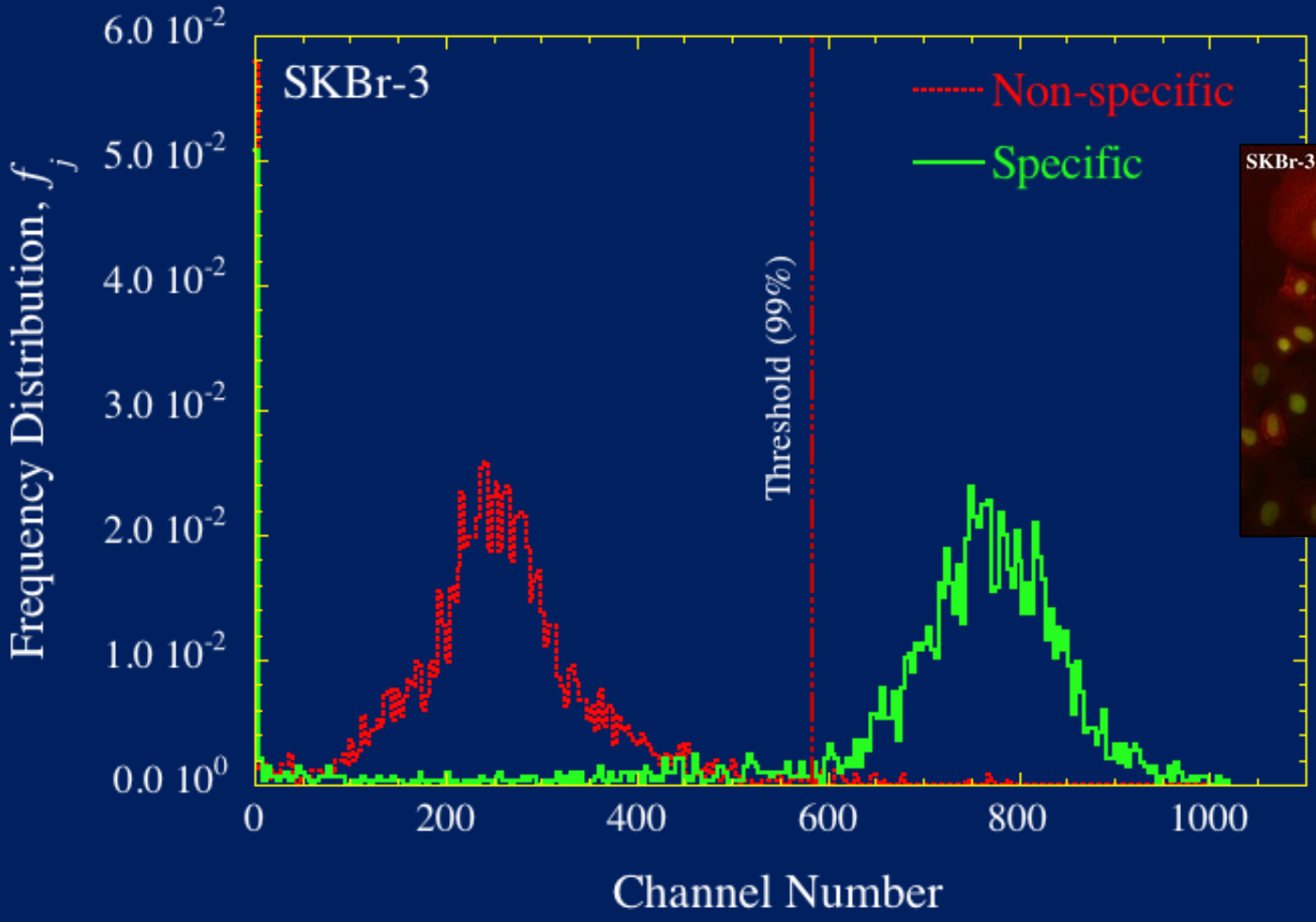

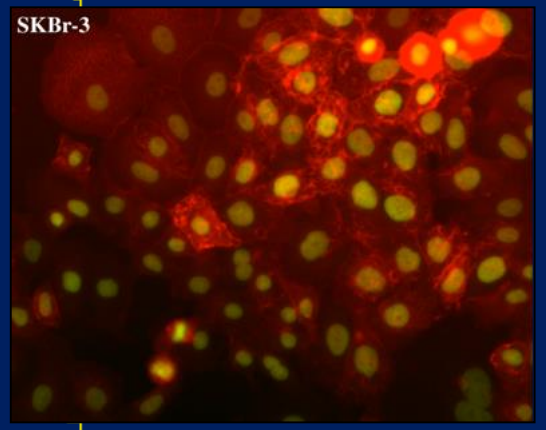

Survival vs Administered Activity SKBr-3

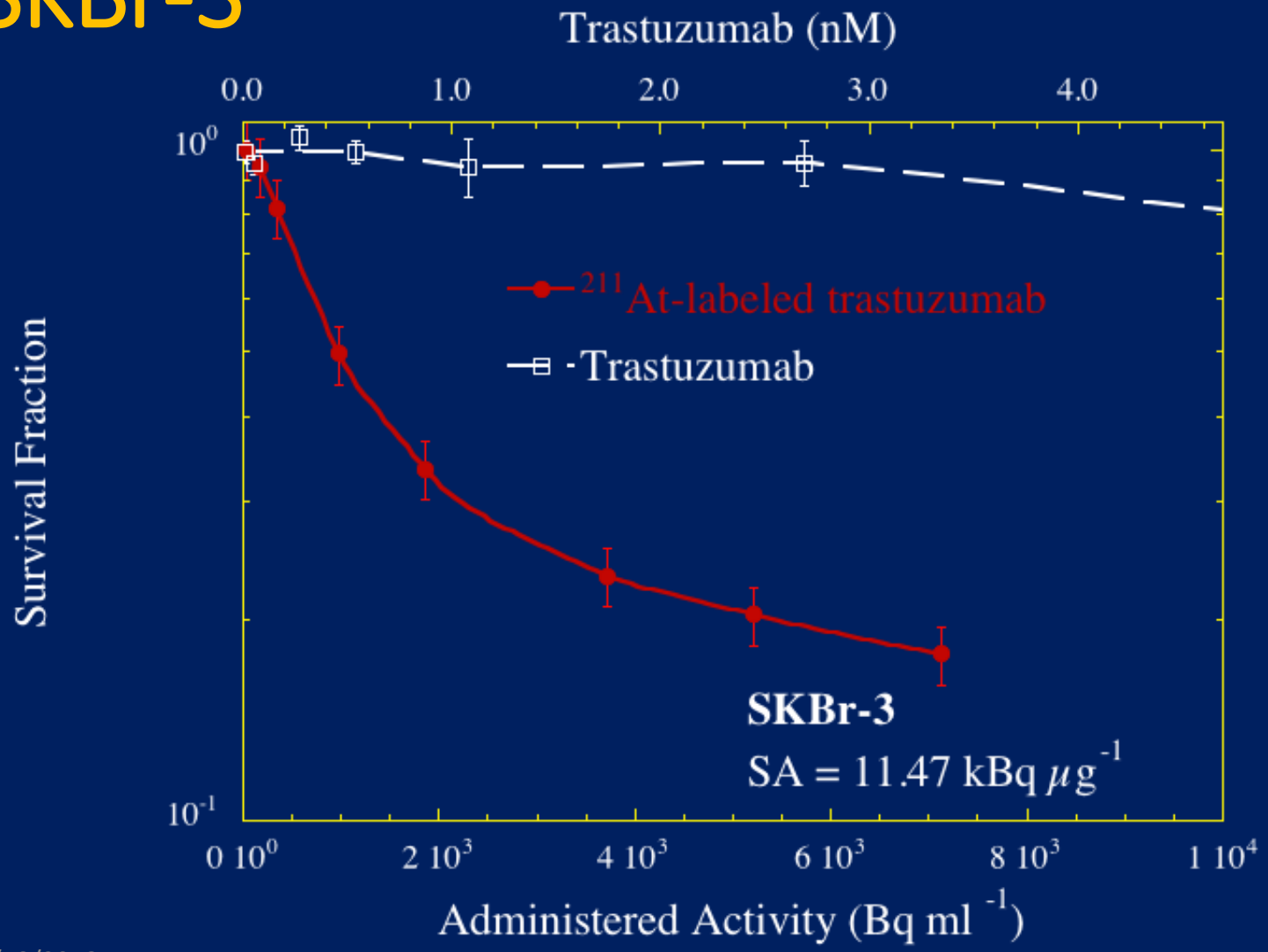

Survival vs Administered Activity MCF-7/HER2-18

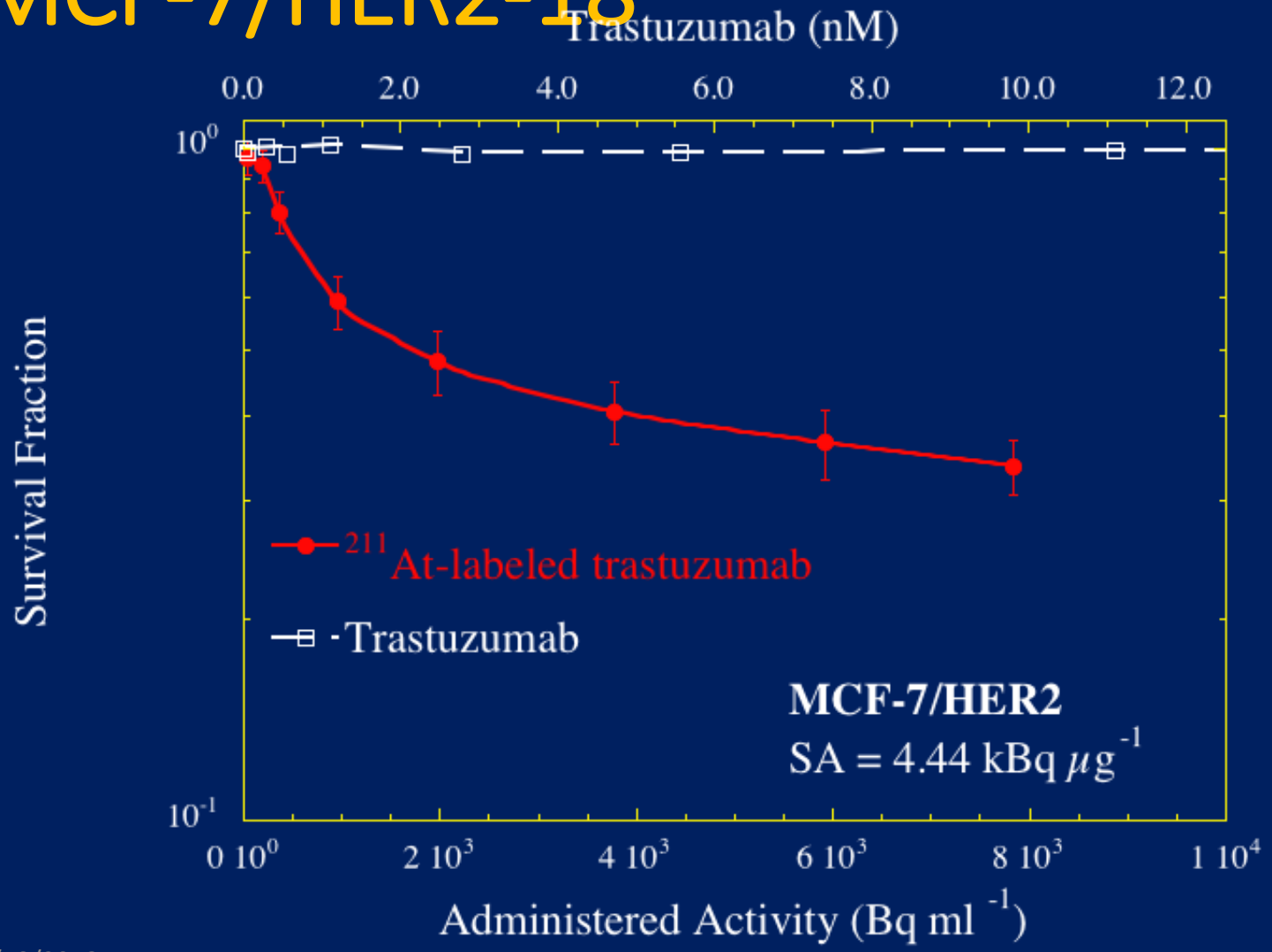

Pharmacokinetic/Microdosimetry Modules

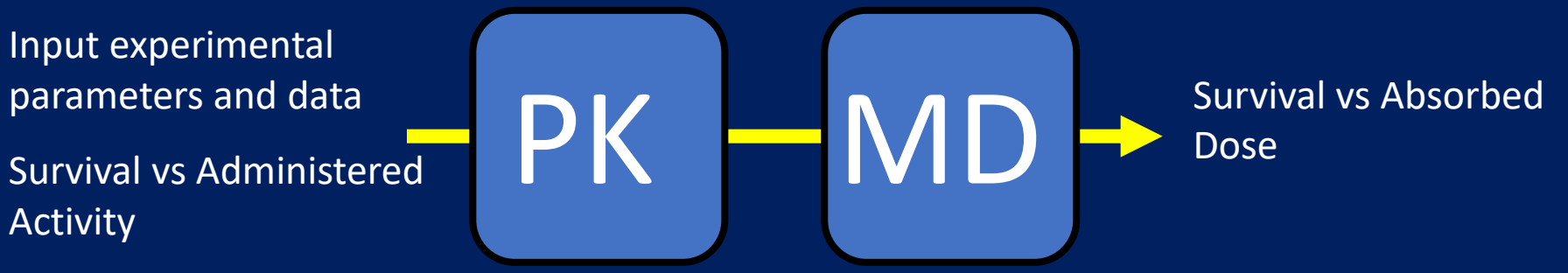

Pharmacokinetic model

Cells are divided into 256 cell groups (*j = 1, …, 256)* based on **FACS** analysis on receptor expression

Initial receptor concentration

$$A_{g0}^{j} = 1 \times 10^{3} \frac{d_c f_j N_{Ag}^{j}}{N_A}$$

Receptor concentration

$$\frac{dA_{g,j}}{dt} = -\frac{dm_{b,j}}{dt}$$

Labeling fraction

$$I_f = 1 \times 10^{6} \frac{SA\, M_W}{\lambda N_A}$$

Estimate the following parameters

- The association, dissociation, and internalization rate constant, k_a, k_d, k_e
- The specific activity, *SA* (kBq μg^{-1})
- The average number of HER-2 receptors per cell, B_{max}

Pharmacokinetic model

Total mAb

Labeled mAb

Unbound mAb

$$\frac{dm_u}{dt} = f_u\left(k_a, k_d, A_{g,j}, m_u, m_b\right)$$

Unbound Labeled mAb

$$\frac{dm'_u}{dt} = I_f\left(\frac{dm_u}{dt} - \lambda m_u\right) e^{-\lambda t}$$

Bound mAb

$$\frac{dm_{b,j}}{dt} = f_{b,j}\left(k_a, k_d, A_{g,j}, m_u, m_{b,j}\right)$$

Bound Labeled mAb

$$\frac{dm'_{b,j}}{dt} = I_f\left(\frac{dm_{b,j}}{dt} - \lambda m_{b,j}\right) e^{-\lambda t}$$

Internalized mAb

$$\frac{dm_{i,j}}{dt} = f_{i,j}\left(k_e, k_x, m_{b,j}, m_{i,j}\right)$$

Internalized Labeled mAb

$$\frac{dm'_{i,j}}{dt} = I_f\left(\frac{dm_{i,j}}{dt} - \lambda m_{i,j}\right) e^{-\lambda t}$$

Microdosimetry Module: Converting Hits into Absorbed Dose

Cell morphology

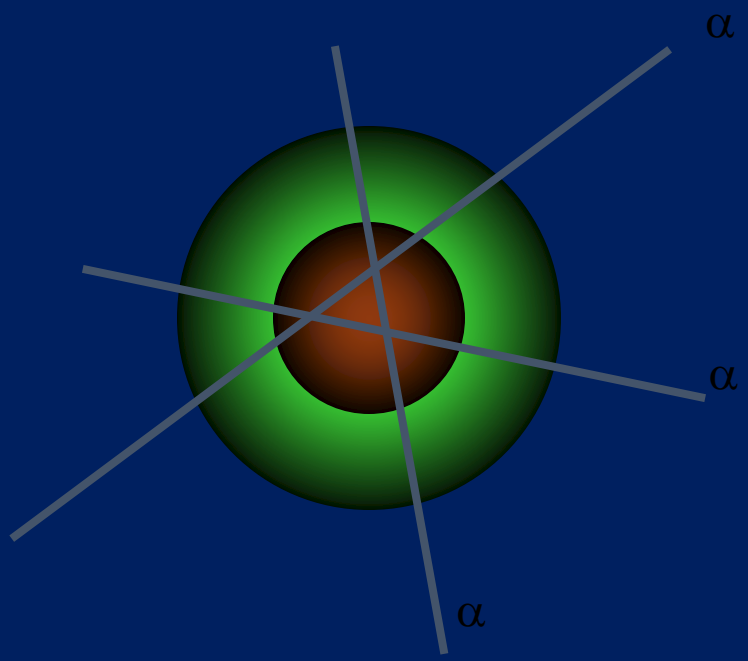

- Medium or Extra-cellular Space
- Cell Surface
- Internalized

Microdosimetry Module: Monte Carlo Transport

Specific energy per event

$$z_i = \frac{\varepsilon_i}{m_h}$$

Average specific energy per event

$$\bar{z}_1 = \frac{1}{N}\sum_{i=1}^{N} z_i$$

Average absorbed dose

$$D = \sum_{i=1}^{n} z_i = \left[h\bar{z}_1\right]_{med} + \left[h\bar{z}_1\right]_{CS} + \left[h\bar{z}_1\right]_{Int}$$

Survival Probability

$$SF = \exp\left(-D/z_0\right)$$

Survival vs Absorbed Dose

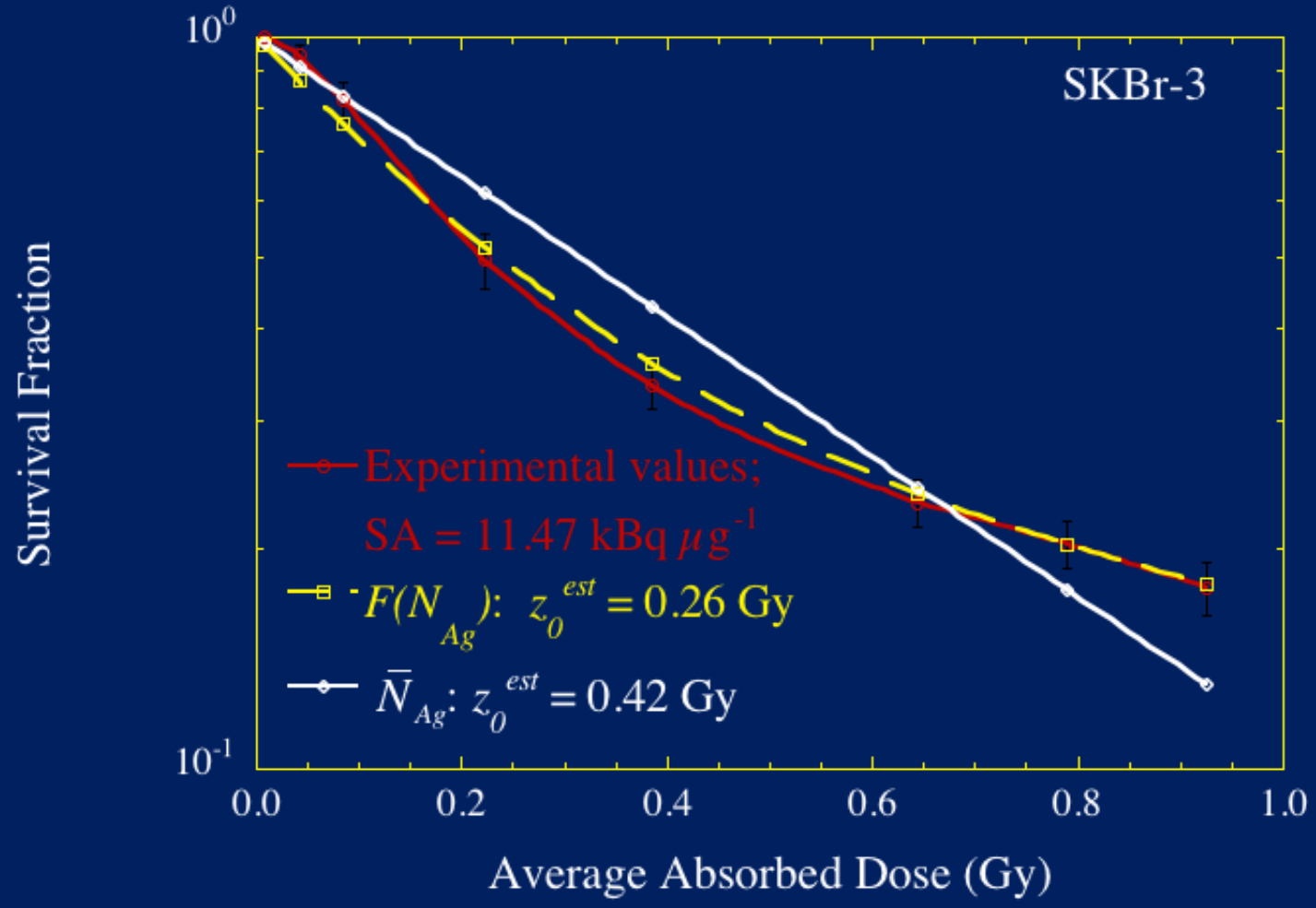

Survival vs Absorbed Dose

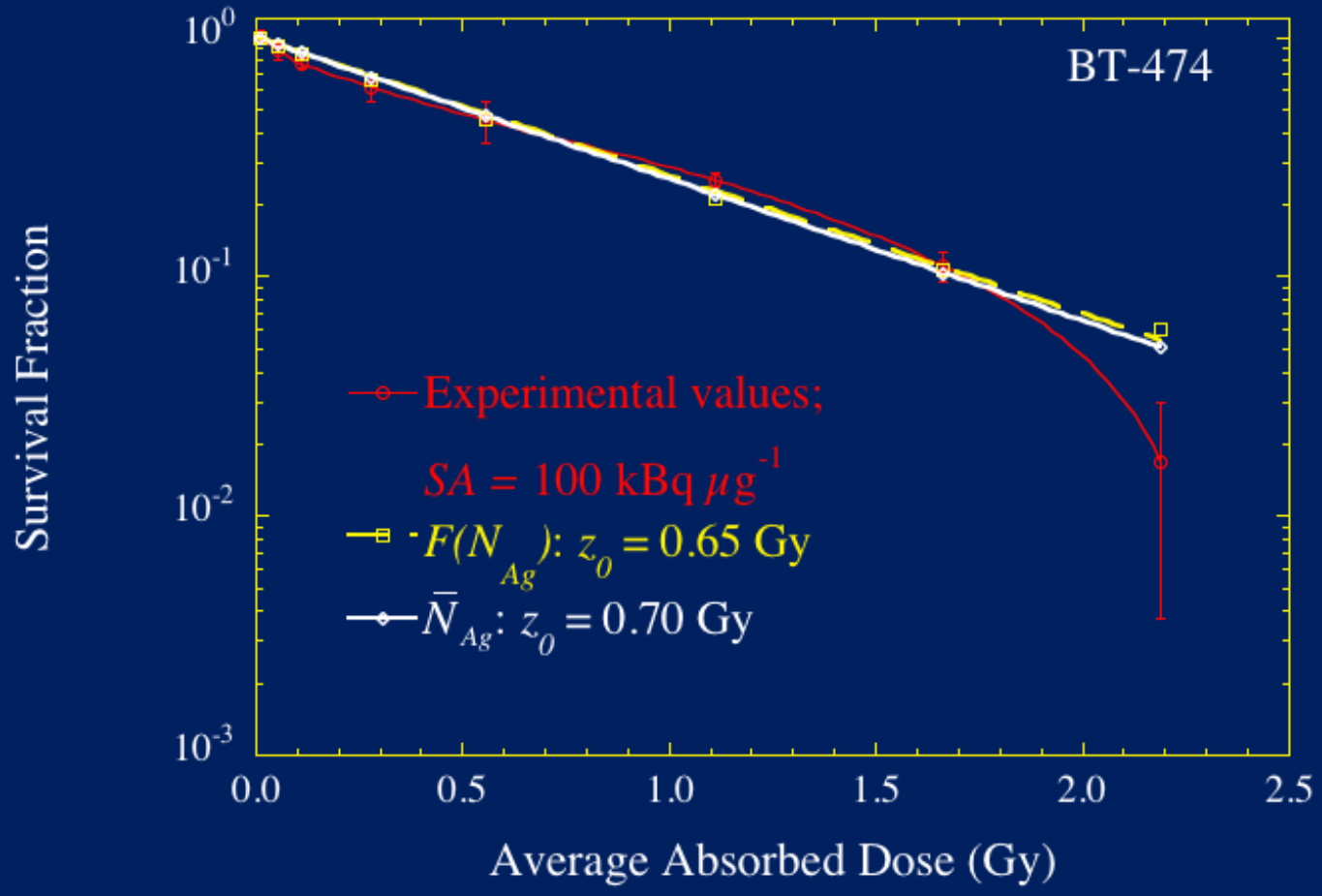

Survival vs Absorbed Dose

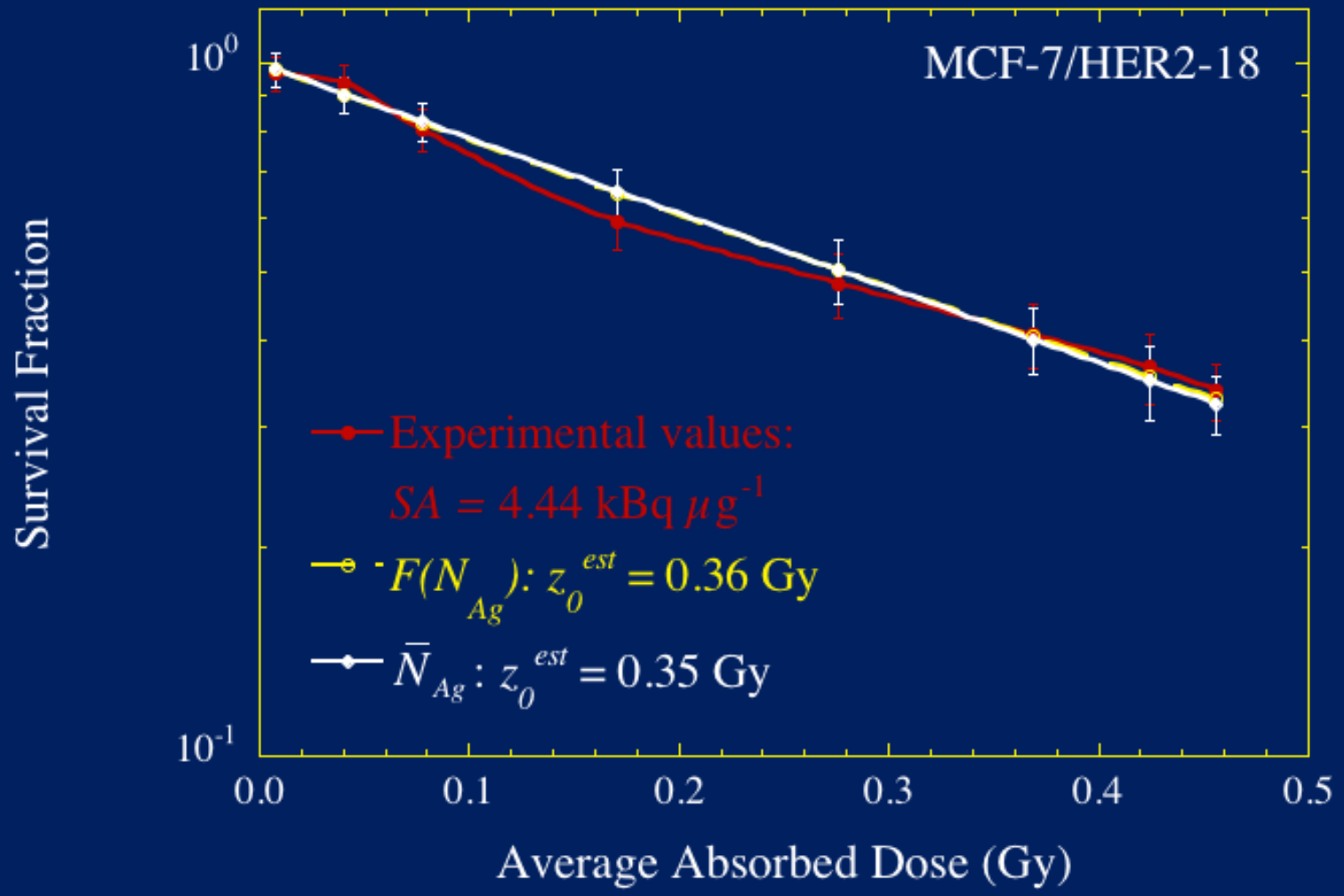

Alpha particle-RIT vs XRT

Cell Line	$D_{37}(Gy)$ XRT	$D_{37}(Gy)$ α-RIT	RBE	$\langle h \rangle$ hits
SKBr-3	2.5	0.26	9.6	4.3
MCF-7/HER2-18	3.1	0.36	8.6	5.6
BT-474	6.1	0.63	9.7	9.4

RBE: Relative Biological Effectiveness
Benefits: localized and specific to HER2-positive tumor cells

In Vivo Preclinical Studies

Organ Biodistribution Studies

- Most preclinical studies carry out organ ex vivo biodistribution studies at different time points and assess gross %ID/g, including tumor.
- Tumor and tissue activity distributions are now estimated using in vivo and ex vivo quantitative imaging methods.
- There is a need to establish high fidelity animal model of human cancers
  - PDX models

The Vascular Physiology Of The Tumor Microenvironment

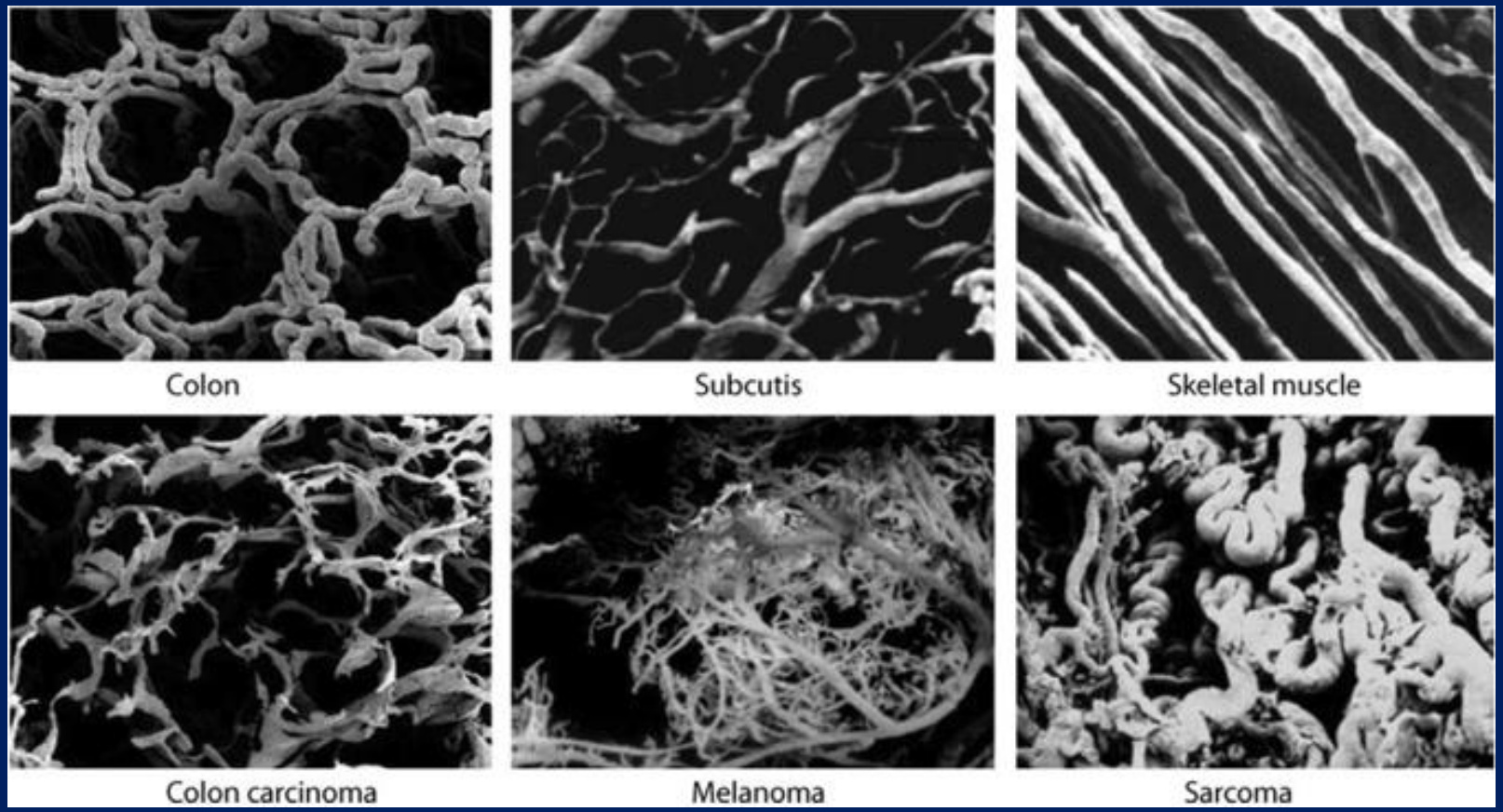

P. Vaupel, "Tumor microenvironmental physiology and its implications for radiation oncology," Semin Radiat Oncol, vol. 14, no. 3, pp. 198–206, Jul. 2004.

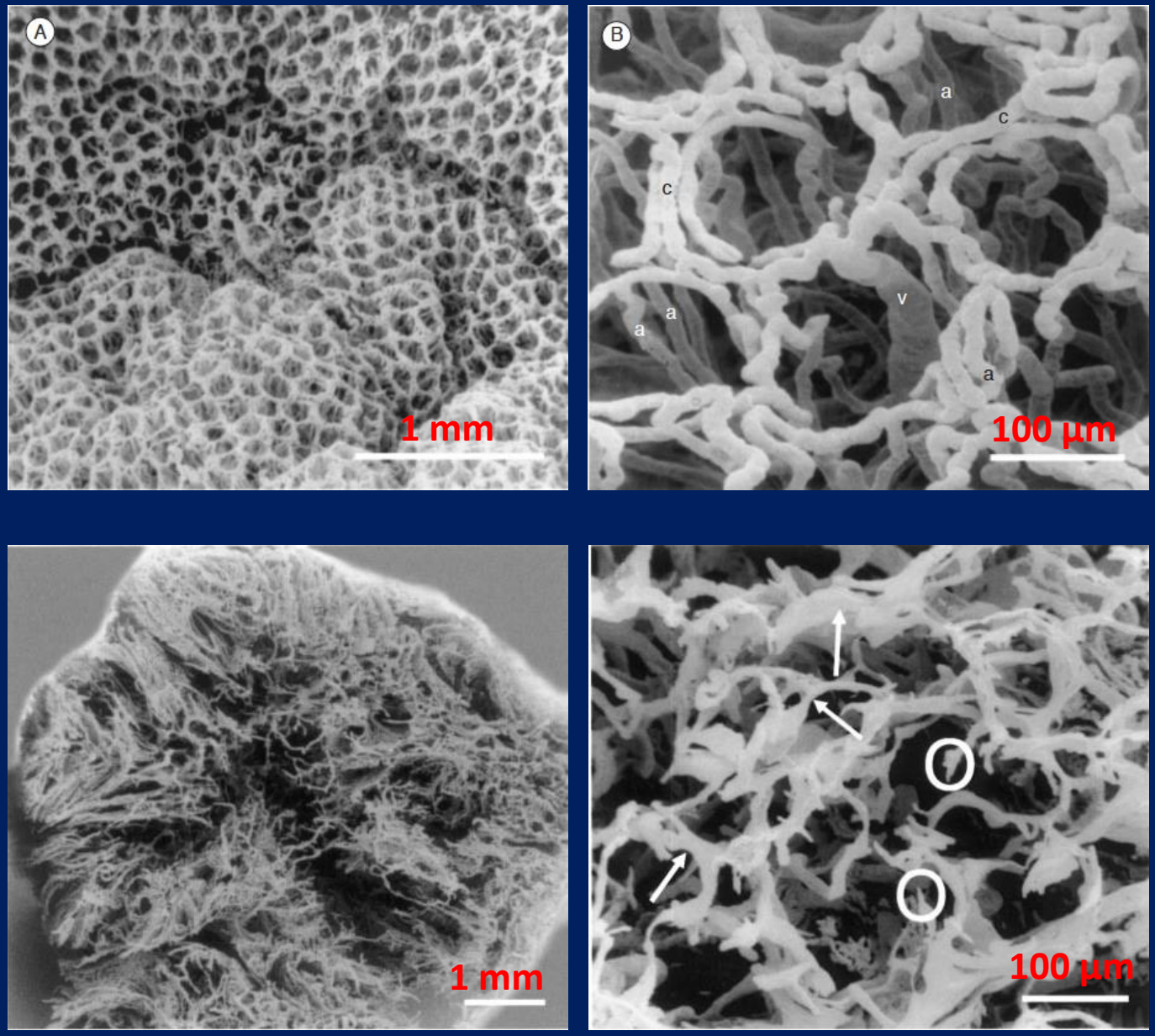

M. A. Konerding, E. Fait, and A. Gaumann, "3D microvascular architecture of pre-cancerous lesions and invasive carcinomas of the colon.," *Br J Cancer*, vol. 84, no. 10, pp. 1354–1362, May 2001.

jove Journal of Visualized Experiments www.jove.com

Video Article

Intravital Microscopy of Tumor-associated Vasculature Using Advanced Dorsal Skinfold Window Chambers on Transgenic Fluorescent Mice

Ann L.B. Seynhaeve[1], Timo L.M. ten Hagen[1]

[1]Laboratory Experimental Surgical Oncology, Section Surgical Oncology, Department of Surgery, Erasmus MC

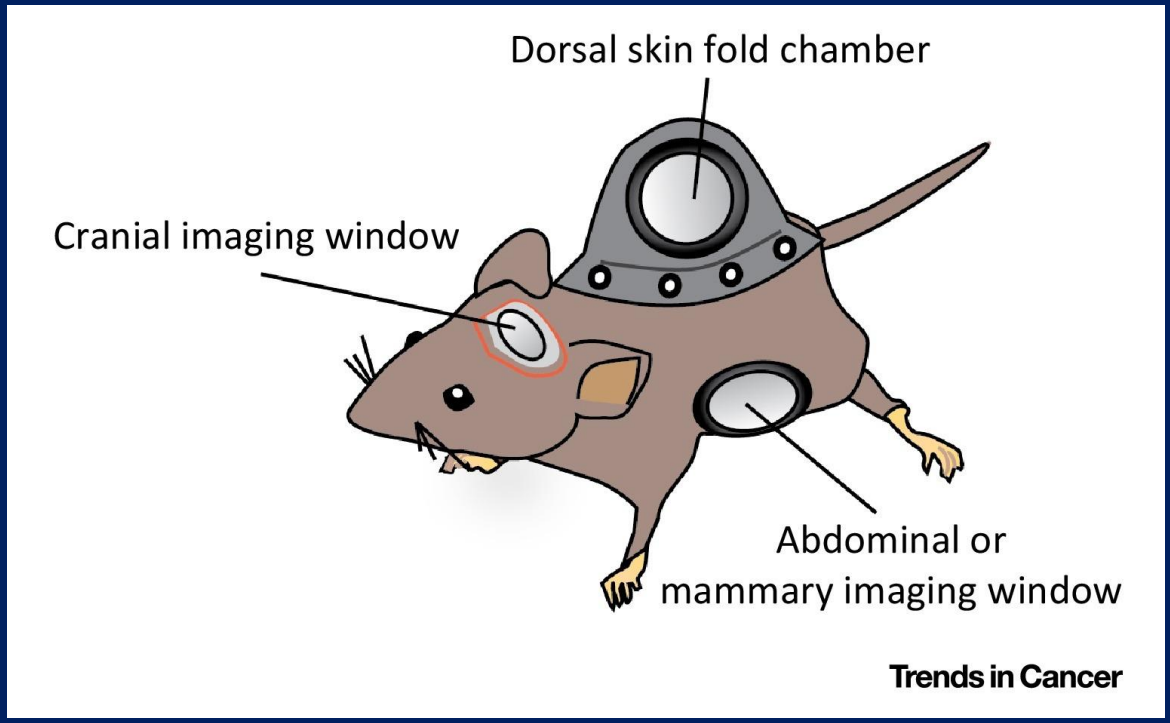

Intrinsically fluorescence endothelial cells

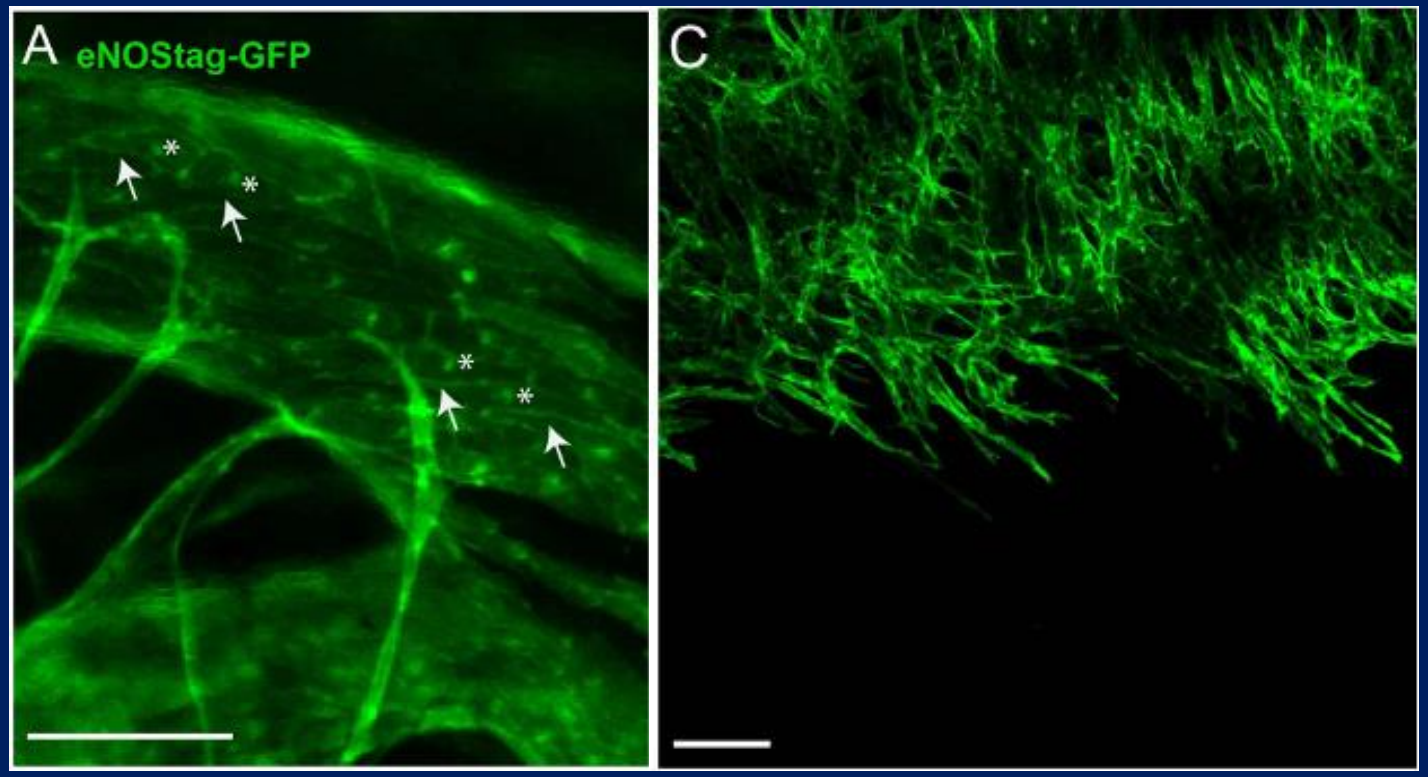
A eNOStag-GFP
C

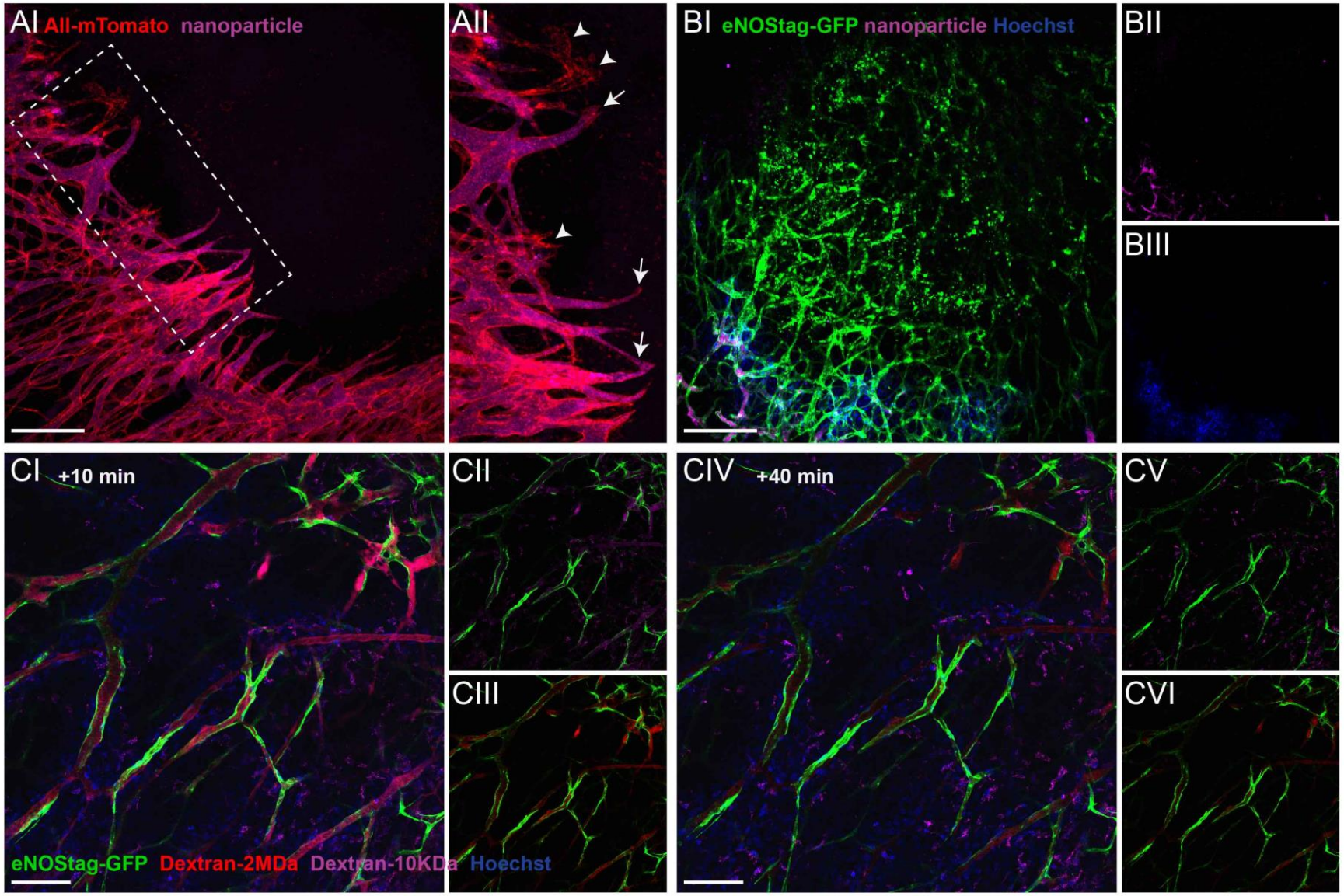
AI AII-mTomato nanoparticle
AII
BI eNOStag-GFP nanoparticle Hoechst
BII
BIII
CI +10 min
CII
CIII
CIV +40 min
CV
CVI
eNOStag-GFP Dextran-2MDa Dextran-10KDa Hoechst

MB PK/PD Models

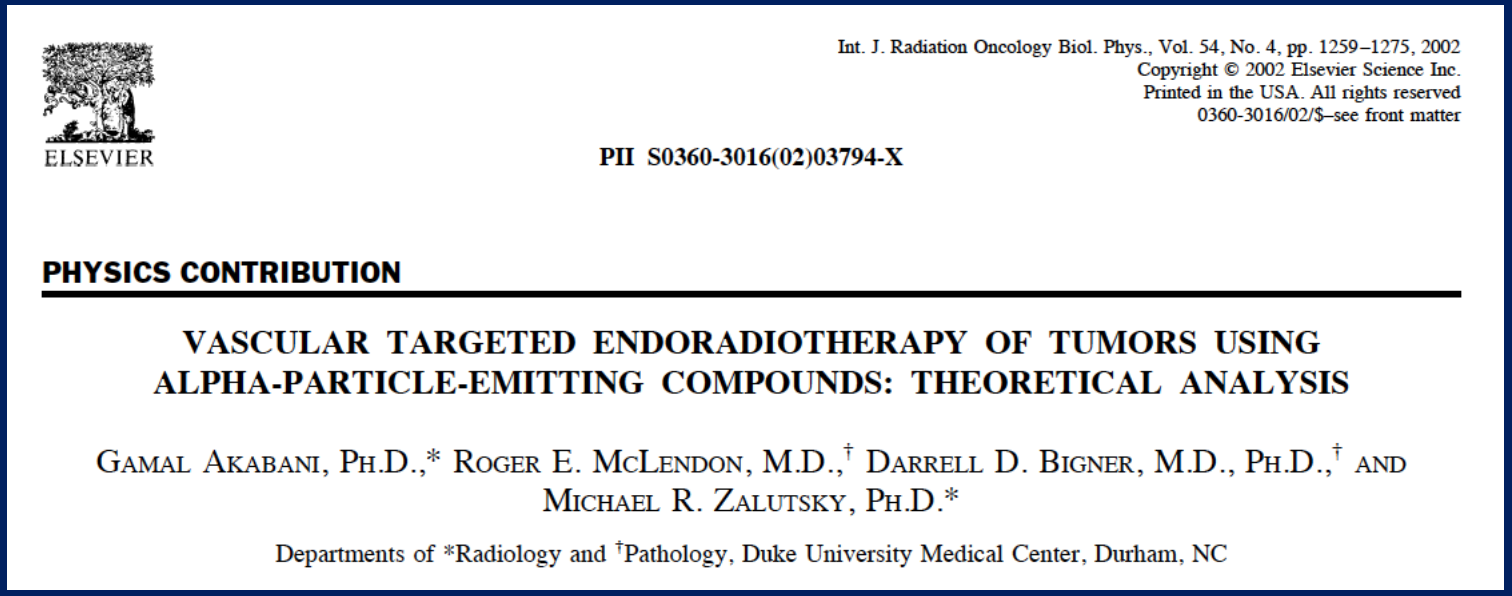

Int. J. Radiation Oncology Biol. Phys., Vol. 54, No. 4, pp. 1259–1275, 2002
Copyright © 2002 Elsevier Science Inc.
Printed in the USA. All rights reserved
0360-3016/02/$–see front matter

PII S0360-3016(02)03794-X

ELSEVIER

PHYSICS CONTRIBUTION

VASCULAR TARGETED ENDORADIOTHERAPY OF TUMORS USING ALPHA-PARTICLE-EMITTING COMPOUNDS: THEORETICAL ANALYSIS

GAMAL AKABANI, PH.D.,* ROGER E. MCLENDON, M.D.,† DARRELL D. BIGNER, M.D., PH.D.,† AND MICHAEL R. ZALUTSKY, PH.D.*

Departments of *Radiology and †Pathology, Duke University Medical Center, Durham, NC

mAb morphological distribution

Autoradiography of I-125 labeled anti-tenascin 81C6 mAb in a glioma animal model

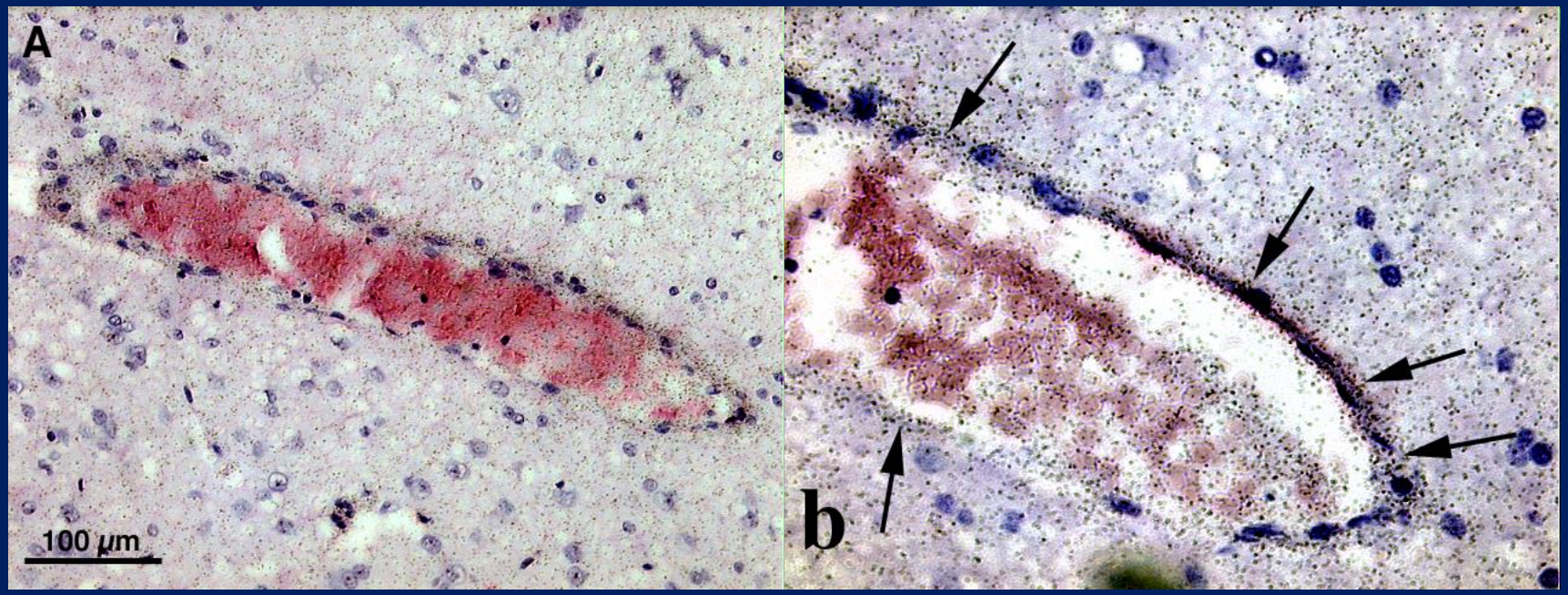

Average Relative Activity Concentration Vessel-to-Blood: 4:1

MB/PK Model

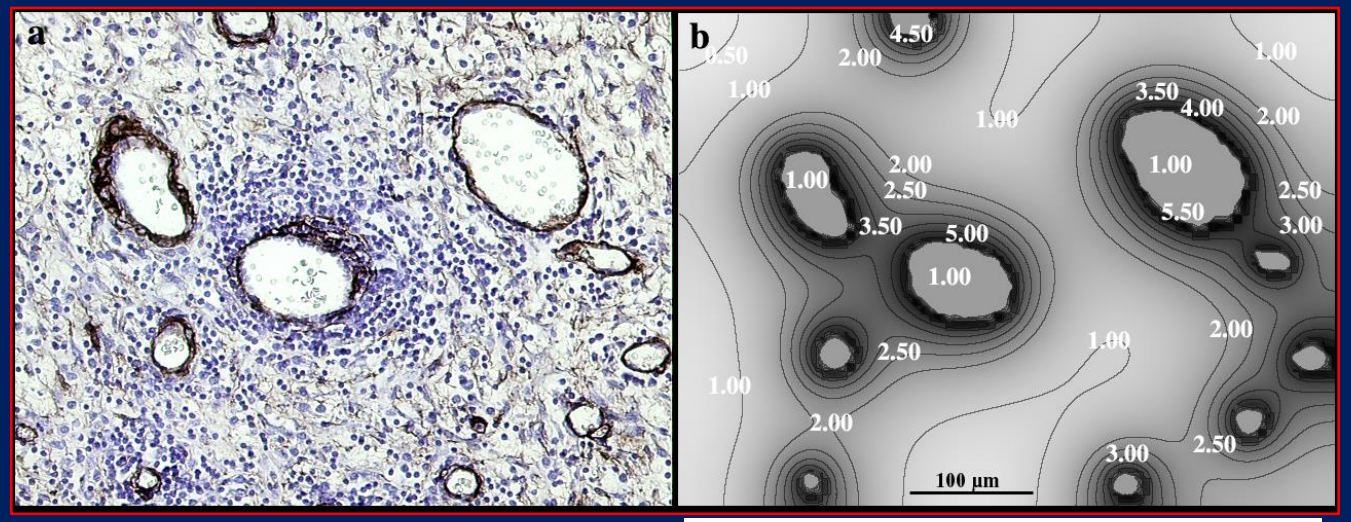

Dose estimates based on convolution methods using a alpha point kernel

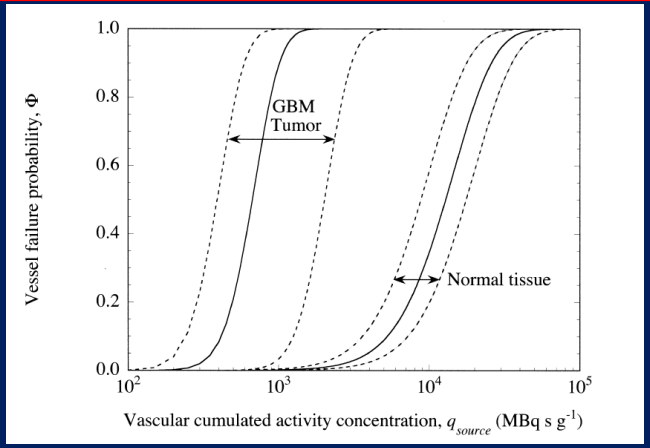

Normalized anti-tenascin 81C6 Mab distribution around tumor vasculature in GBM tumors

MB/PK Microdosimetry

Vascular Targeted Radioimmunotherapy for the Treatment of Glioblastoma

Katja Behling[1], William F. Maguire[2], José Carlos López Puebla[1], Shanna R. Sprinkle[1], Alessandro Ruggiero[1], Joseph O'Donoghue[3], Philip H. Gutin[4,5], David A. Scheinberg[2,6], and Michael R. McDevitt[1,7]

[1]Department of Radiology, Memorial Sloan Kettering Cancer Center, New York, New York; [2]Department of Molecular Pharmacology, Memorial Sloan Kettering Cancer Center, New York, New York; [3]Department of Medical Physics, Memorial Sloan Kettering Cancer Center, New York, New York; [4]Department of Neurosurgery, Memorial Sloan Kettering Cancer Center, New York, New York; [5]Department of Neurological Surgery, Weill Cornell Medical College, New York, New York; [6]Department of Pharmacology, Weill Cornell Medical College, New York, New York; and [7]Department of Medicine, Weill Cornell Medical College, New York, New York

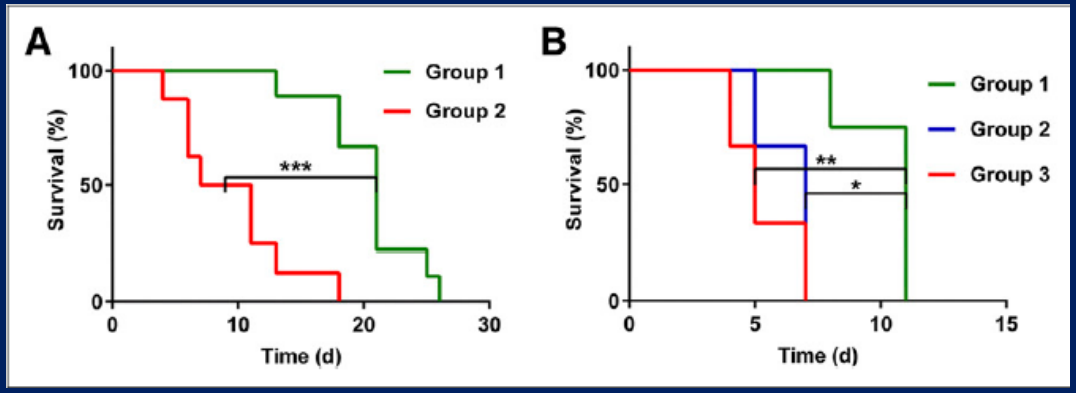

Ex Vivo Alpha Particle imaging using histological samples

- Alpha Camera - Sweden
- iQID Camera - PNNL/ University of Arizona
- Timepix Detector - Australia
- Small scale dosimetry
  - Staking of histological slides for dose convolution methods
  - Need for superposition with immunohistochemistry tissues
- Tissue sectioning has disadvantages when investigating dynamic processes

Ex Vivo small-scale dosimetry

Ex Vivo Activity Quantification in Micrometastases at the Cellular Scale Using the α-Camera Technique

Nicolas Chouin[1,2], Sture Lindegren[2], Sofia H.L. Frost[2], Holger Jensen[3], Per Albertsson[4], Ragnar Hultborn[4], Stig Palm[2], Lars Jacobsson[2], and Tom Bäck[2]

[1]LUNAM Université, Oniris, AMaROC, Nantes, France; [2]Department of Radiation Physics, Institute of Clinical Sciences, Sahlgrenska Academy, University of Gothenburg, Gothenburg, Sweden; [3]Cyclotron and PET Unit, Rigshospitalet, Copenhagen, Denmark; and [4]Department of Oncology, Institute of Clinical Sciences, Sahlgrenska Academy, University of Gothenburg, Gothenburg, Sweden

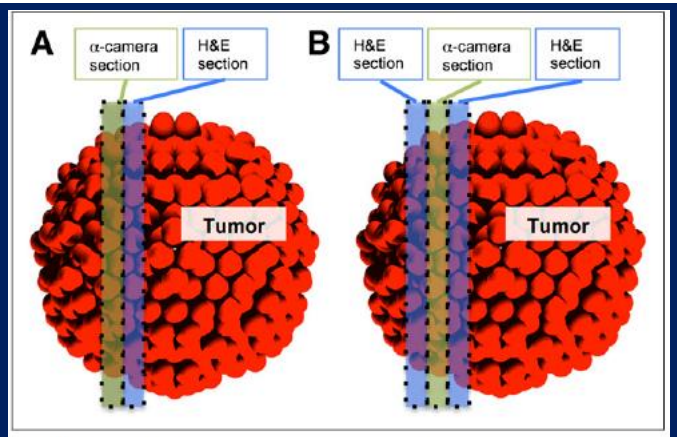

FIGURE 2. Description of sectioning scheme performed on biologic samples. (A) Method for all biologic samples: first section was used for α-camera imaging and consecutive section for H&E staining. In some cases, 3 consecutive sections were taken (B) to evaluate accuracy of cell number determination.

In Situ Dosimetry

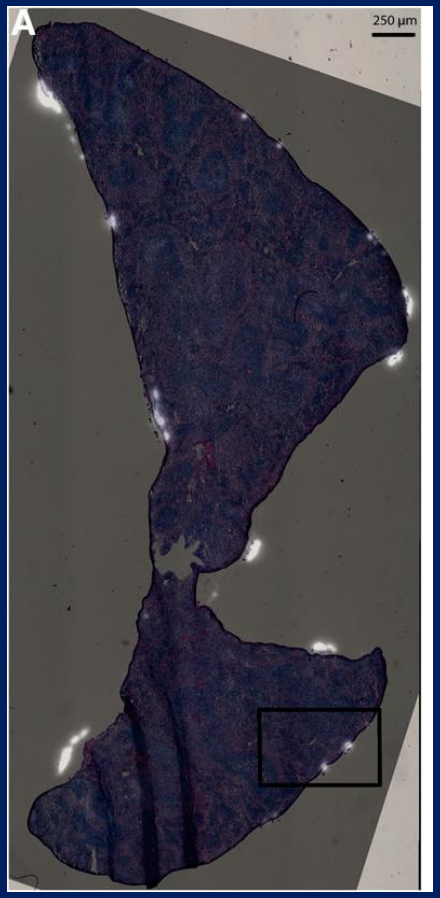

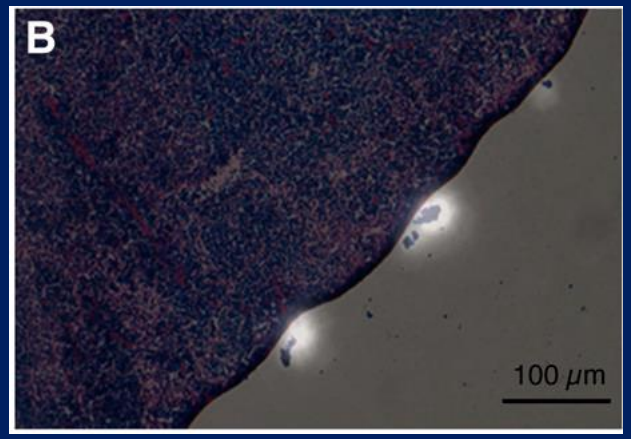

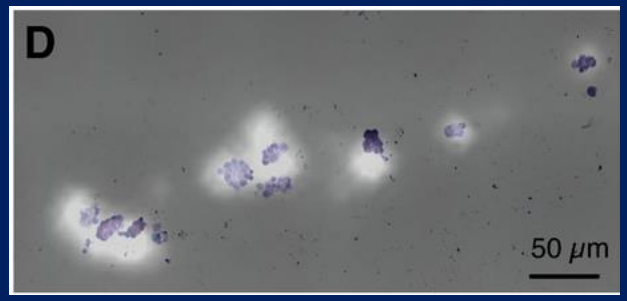

Estimated absorbed doses were about 40 and 12 Gy for large (23 – 43 µm) and small (<13 µm) tumor foci

In Vivo Imaging

- There are limitations in using the alpha camera in carrying out single-animal longitudinal studies.
- There is the need for long-term longitudinal studies where each animal is its own control.
- Better estimations of the residence time in organs at risk, blood and bone marrow and other regions including tumor.

Physics in Medicine & Biology

IPEM Institute of Physics and Engineering in Medicine

PAPER

Evaluation of ^{209}At as a theranostic isotope for ^{209}At-radiopharmaceutical development using high-energy SPECT

RECEIVED
27 September 2017

REVISED
18 December 2017

ACCEPTED FOR PUBLICATION
25 January 2018

PUBLISHED
21 February 2018

J R Crawford[1,2,3,8], A K H Robertson[1,4,8], H Yang[1], C Rodríguez-Rodríguez[4,5], P L Esquinas[6], P Kunz[7], S Blinder[4], V Sossi[4], P Schaffer[1,6] and T J Ruth[1,3]

1 Life Sciences Division, TRIUMF, 4004 Wesbrook Mall, Vancouver BC, V6T 2A3, Canada
2 Molecular Oncology, BC Cancer Research Centre, 675 W 10th Ave, Vancouver BC, V5Z 1L3, Canada
3 Department of Physics and Astronomy, University of Victoria, PO Box 1700 STN CSC, Victoria BC, V8W 2Y2, Canada
4 Department of Physics and Astronomy, University of British Columbia (UBC), 6224 Agronomy Road, Vancouver BC, V6T 1Z1, Canada
5 Centre for Comparative Medicine, University of British Columbia (UBC), 4145 Wesbrook Mall, Vancouver BC, V6T 1W5, Canada
6 Department of Radiology, University of British Columbia, 3350-950 W 10th Ave, Vancouver BC, V5Z 4E3, Canada
7 Accelerator Division, TRIUMF, 4004 Wesbrook Mall, Vancouver BC, V6T 2A3, Canada
8 Equal contributors.

E-mail: jcrawford@bccrc.ca

Keywords: astatine-211, astatine-209, theranostic pair, preclinical imaging, SPECT

At-209 as a Theranostic Isotope

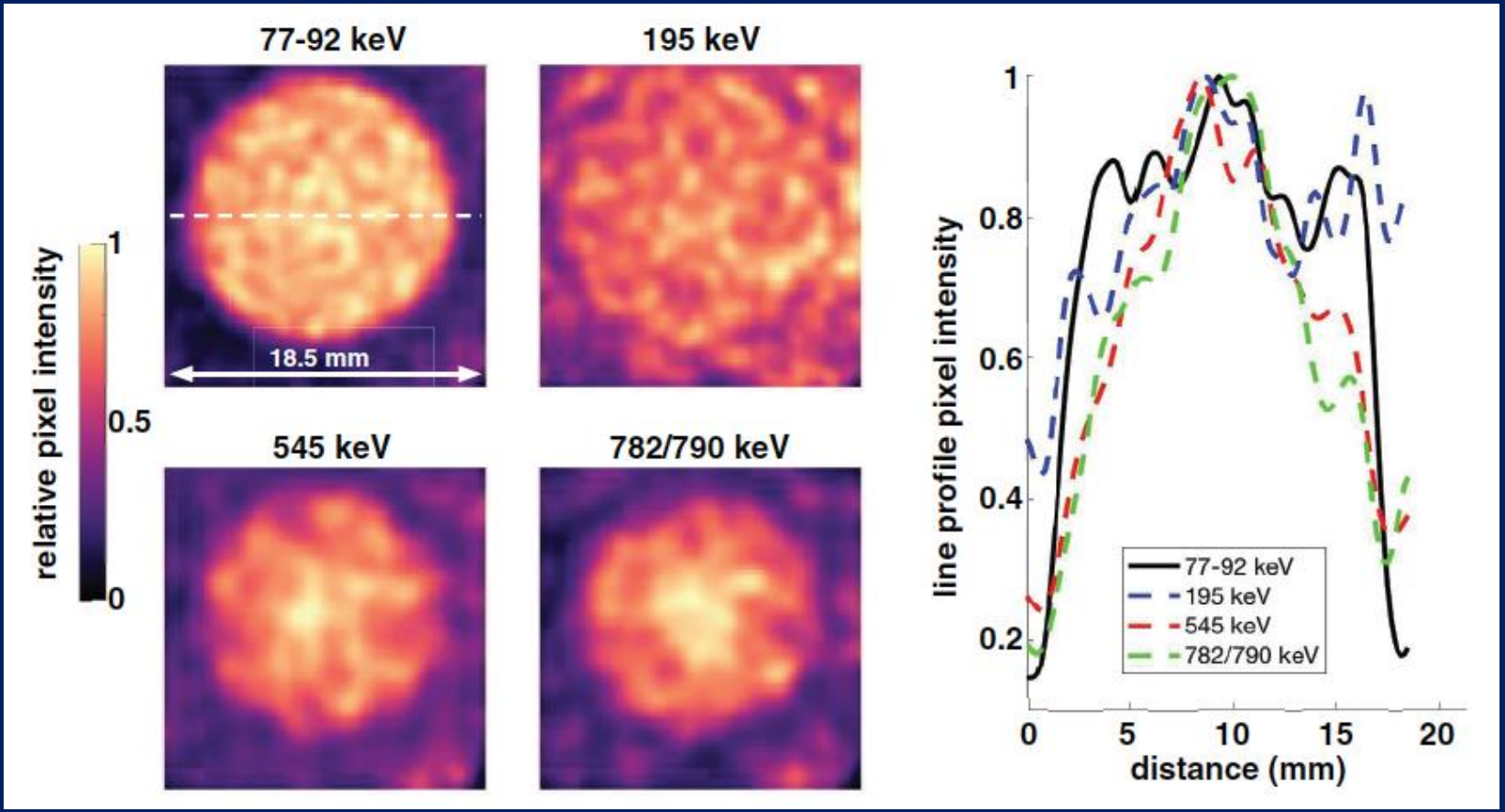

J. R. Crawford, A. K. H. Robertson, H. Yang, C. Rodríguez-Rodríguez, P. L. Esquinas, P. Kunz, S. Blinder, V. Sossi, P. Schaffer, and T. J. Ruth, "Evaluation of 209At as a theranostic isotope for 209At-radiopharmaceutical development using high-energy SPECT.," *Physics In Medicine And Biology*, vol. 63, no. 4, pp. 045025–, Feb. 2018.

MIP Imaging of Free At-209

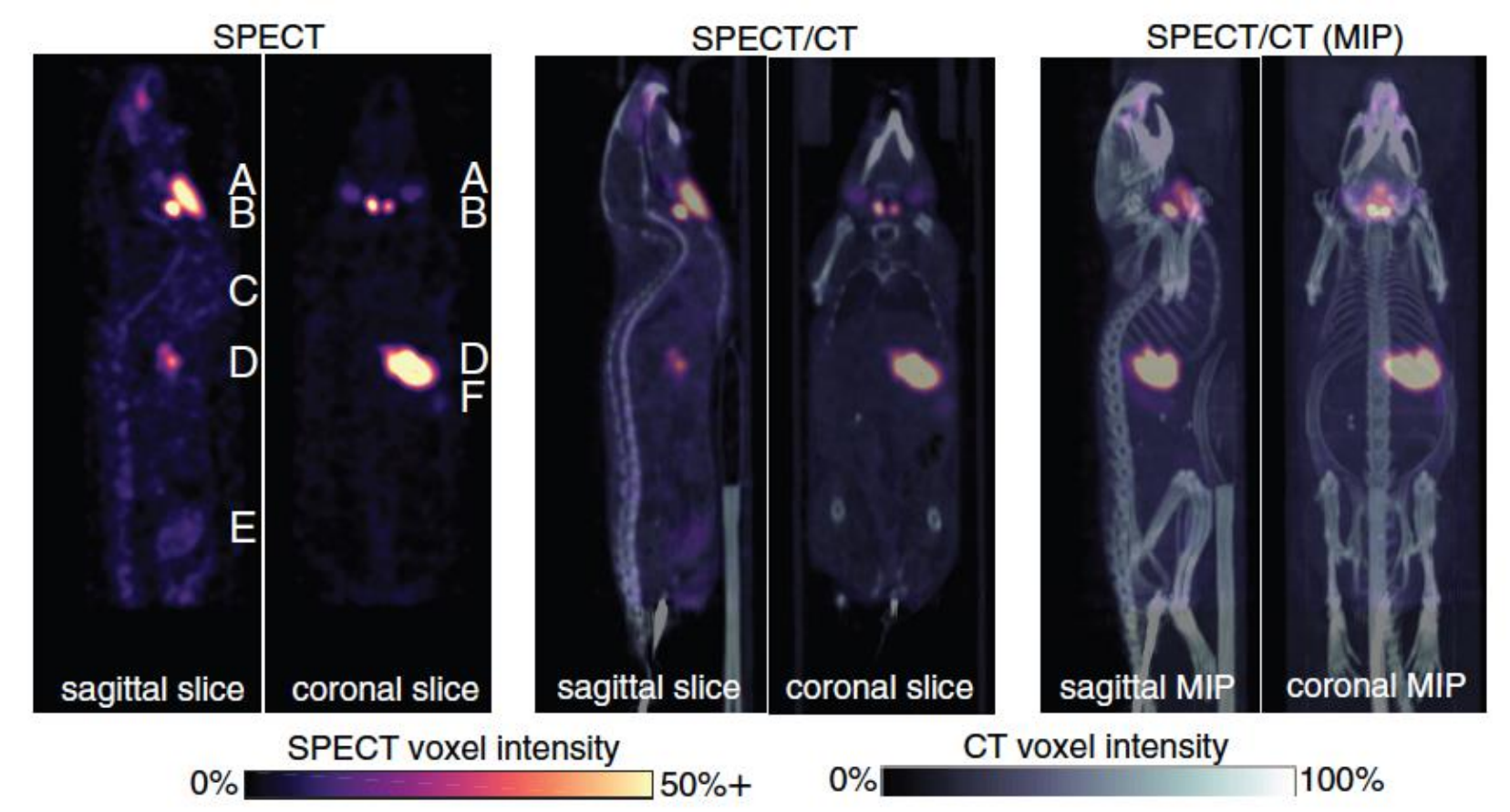

HE Collimator with 162 focused pinhole apertures (77–92 keV x-rays). Voxel size: 169 µm.

Dynamic SPECT and Ex-Vivo Data

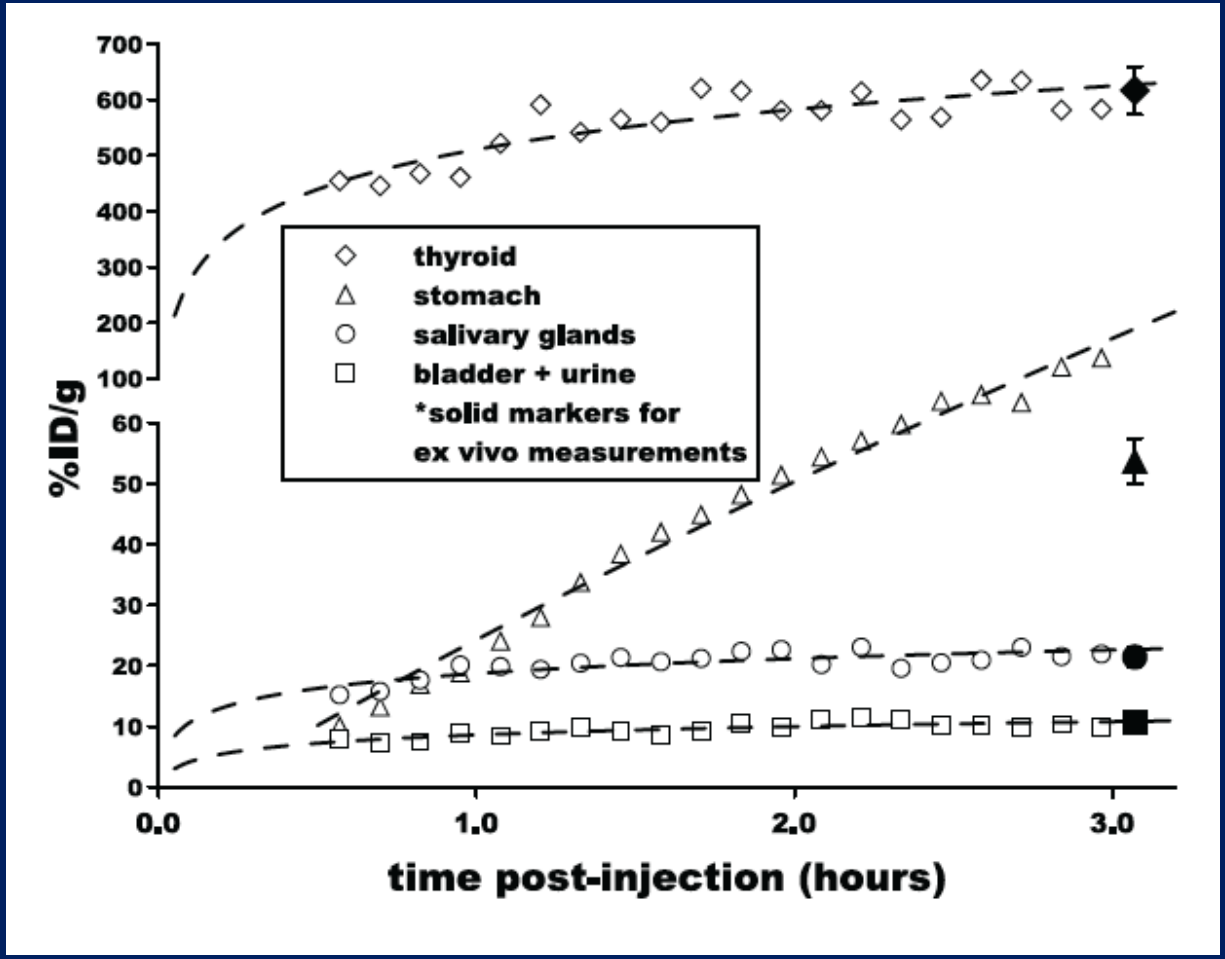

The Combination

- Micro-structural data of tumor morphology and dynamics
- Quantitative imaging of histological slides using an alpha camera
- In Vivo quantitative imaging using a surrogate radionuclide
- Excellent opportunity to study and address the spatiotemporal distribution and effects of alpha particle therapeutics

Clinical Studies

Clinical Experience with α-Particle–Emitting ^{211}At: Treatment of Recurrent Brain Tumor Patients with ^{211}At-Labeled Chimeric Antitenascin Monoclonal Antibody 81C6

Michael R. Zalutsky[1,2], David A. Reardon[2,3], Gamal Akabani[1], R. Edward Coleman[1], Allan H. Friedman[2,4], Henry S. Friedman[2,4], Roger E. McLendon[2,5], Terence Z. Wong[1], and Darell D. Bigner[2,5]

[1]Department of Radiology, Duke University Medical Center, Durham, North Carolina; [2]The Preston Robert Tisch Brain Tumor Center, Duke University Medical Center, Durham, North Carolina; [3]Department of Medicine, Duke University Medical Center, Durham, North Carolina; [4]Department of Surgery, Duke University Medical Center, Durham, North Carolina; and [5]Department of Pathology, Duke University Medical Center, Durham, North Carolina

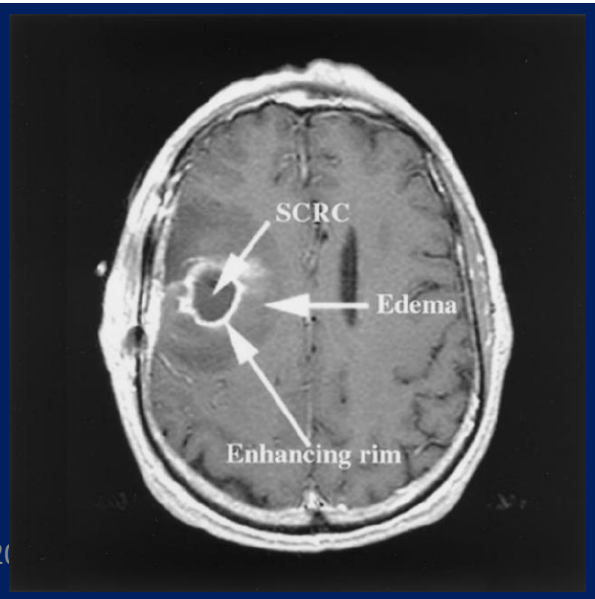

Patient Characteristics

TABLE 1
Pharmacokinetics and Overall Survival and Toxicity Results for Patients Treated with ^{211}At-ch81C6

Patient	Histologic findings	Administered activity (MBq)	Cavity volume (cm^3)	Cavity residence time (h)	% of decays occurring in cavity	%ID in blood pool at: 6 h	%ID in blood pool at: 12 h	Overall survival (wk)	Toxicity*
1	AO	72.7	6.0	10.3	99.0	0.018	0.055	235	
2	GBM	74.0	21.7	10.0	96.0	0.020	0.064	59	
3	GBM	70.7	3.7	9.7	93.3	0.106	0.261	82	Aplastic anemia (grade 4); seizures (grade 3)
4	GBM	72.2	2.4	10.4	100.0	NA	NA	42	Hand numbness (grade 2; resolved)
5	AO	103.6	10.0	10.2	98.0	NA	NA	116	Seizures (grade 3); headache (grade 2; resolved)
6	GBM	144.3	0.2	10.3	99.0	NA	NA	150	Seizures (grade 3)
7	GBM	144.7	15.3	10.3	99.0	0.044	0.093	151	
8	GBM	135.4	9.5	10.3	99.0	0.023	0.038	46	
9	GBM	148.0	29.5	9.8	94.1	NA	NA	54	Seizures (grade 2); headache (grade 2; resolved); visual field loss (grade 2)
10	GBM	148.0	15.2	10.2	98.0	NA	NA	51	Aphasia (grade 2; resolved)
11	GBM	148.0	16.0	10.1	97.1	NA	NA	14	
12	GBM	245.3	37.2	9.8	94.1	0.010	0.019	25	
13	GBM	236.4	2.4	9.6	92.2	0.174	0.430	53	
14	GBM	247.9	7.4	9.6	92.2	0.013	0.019	32	
15	GBM	236.8	11.9	9.1	87.4	0.077	0.122	15	Seizures (grade 4)
16	AO	214.6	28.3	10.4	100.0	NA	NA	71	
17	GBM	347.1	33.9	10.4	100.0	0.027	0.037	76	Headache (grade 2; resolved)
18	AA	148.0	4.8	10.3	99.0	NA	NA	78	Seizures (grade 2)

*Toxicity grade in accordance with CTC version 2.0.
NA = not available.

Whole-Body Imaging

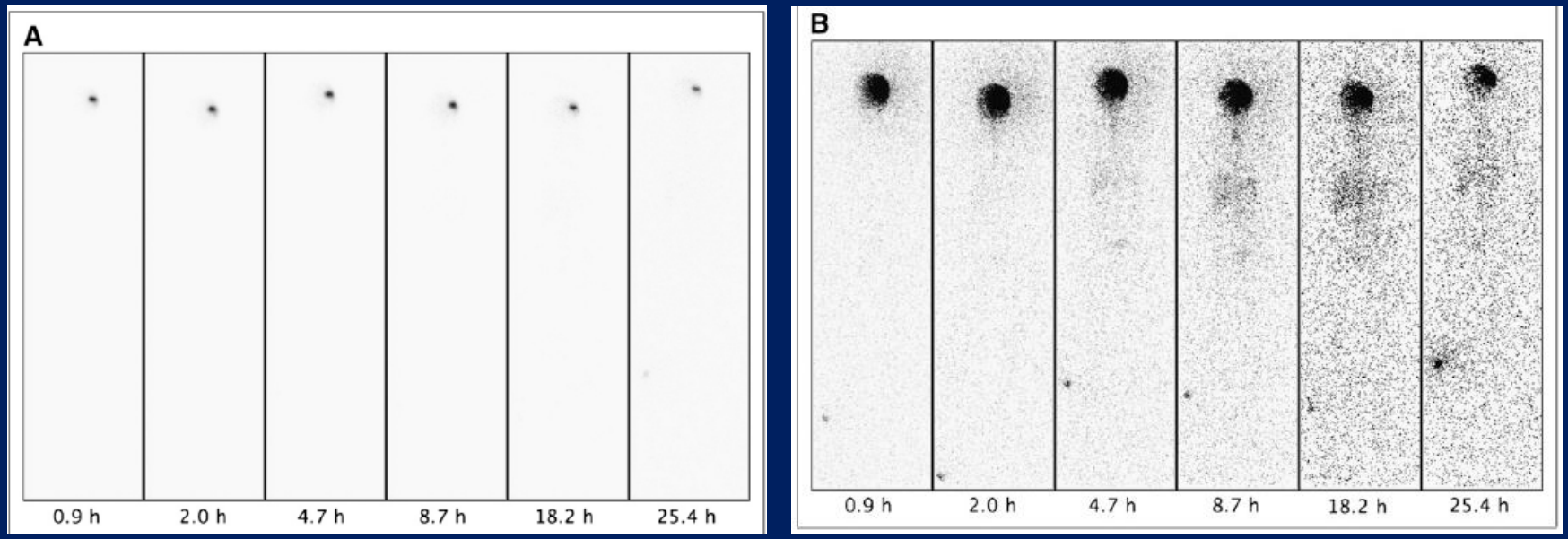

Serial whole-body anterior **g**-camera images obtained after injection of 73 MBq of 211At-ch81C6 into SCRC of patient 1. (A) 100% window. (B) 1% window set to enhance areas with low activity concentrations. Focal activity seen in lower part of image is imaging standard.

Estimated Absorbed Doses to the Cavity Interface

Patient	Histology	Dose (Gy)
1	AO	49
2	GBM	14
3	GBM	78
4	GBM	123
5	AO	42
6	GBM	2938
7	GBM	39
8	GBM	58
9	GBM	20
10	GBM	40
11	GBM	38
12	GBM	27
13	GBM	401
14	GBM	136
15	GBM	81
16	AO	31
17	GBM	42
18	AA	126

Average absorbed dose : 240 Gy
Median Survival of 54.1 weeks.
No limiting toxicity was reached

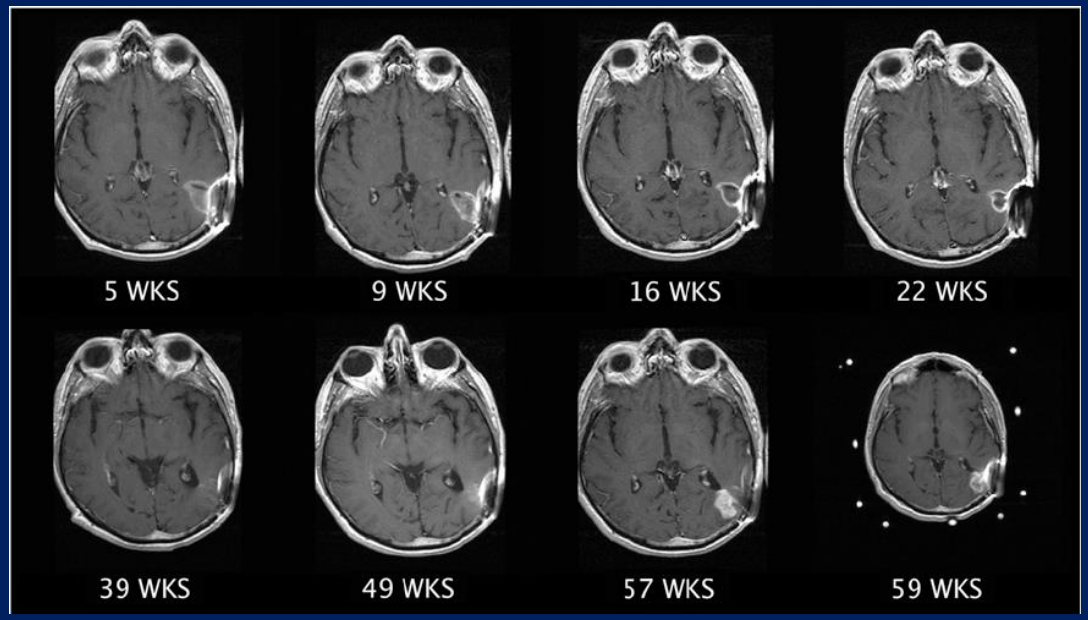

Intraperitoneal α-Particle Radioimmunotherapy of Ovarian Cancer Patients: Pharmacokinetics and Dosimetry of ^{211}At-MX35 F(ab′)$_2$—A Phase I Study

Håkan Andersson[1], Elin Cederkrantz[2], Tom Bäck[2], Chaitanya Divgi[3], Jörgen Elgqvist[1], Jakob Himmelman[2], György Horvath[1], Lars Jacobsson[2], Holger Jensen[4], Sture Lindegren[2], Stig Palm[2], and Ragnar Hultborn[1]

[1]Department of Oncology, University of Gothenburg, Gothenburg, Sweden; [2]Department of Radiation Physics, University of Gothenburg, Gothenburg, Sweden; [3]Hospital of the University of Pennsylvania, Philadelphia, Pennsylvania; and [4]PET and Cyclotron Unit, Rigshospitalet, Copenhagen, Denmark

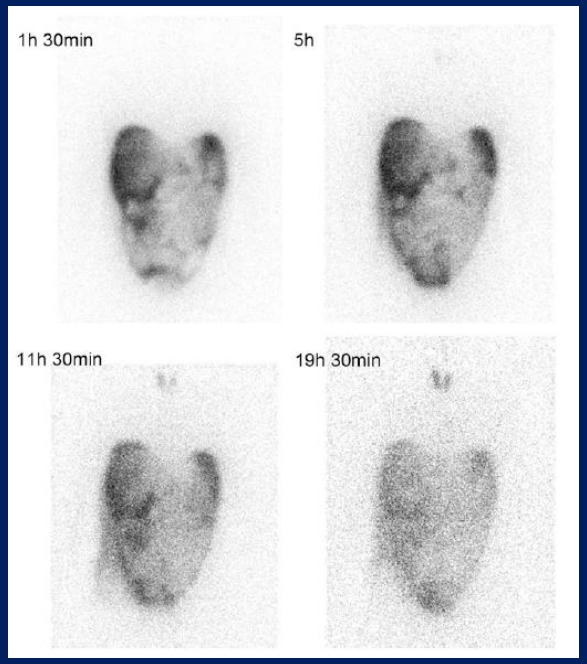

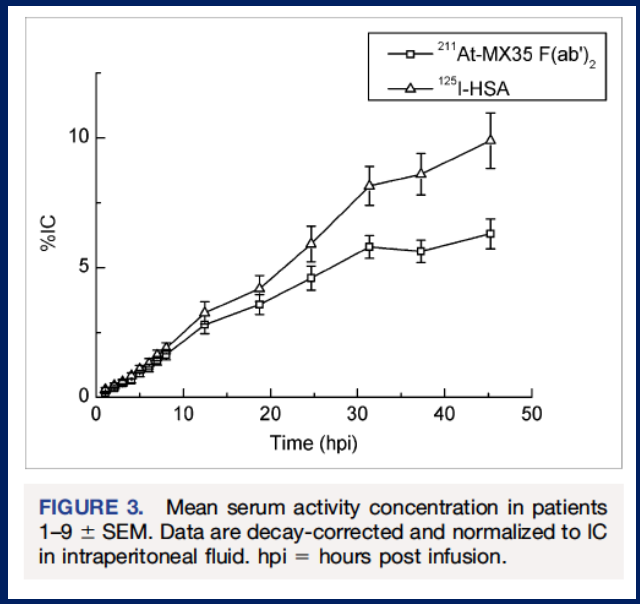

FIGURE 3. Mean serum activity concentration in patients 1–9 ± SEM. Data are decay-corrected and normalized to IC in intraperitoneal fluid. hpi = hours post infusion.

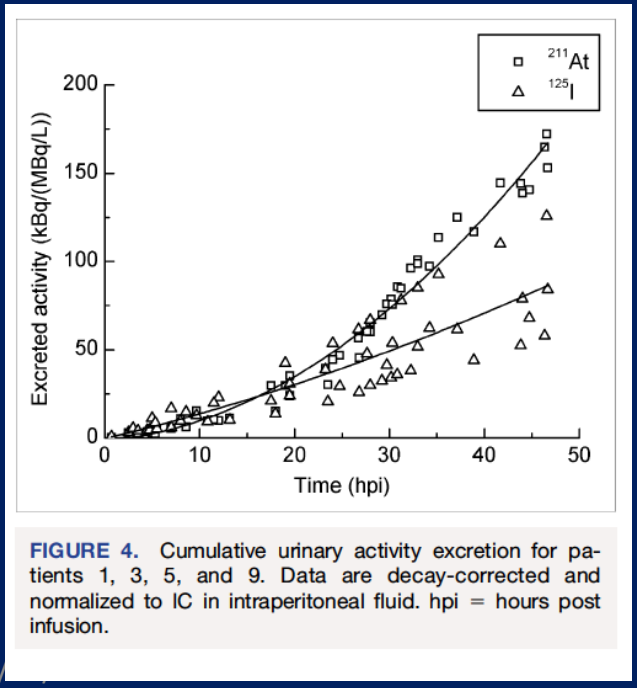

FIGURE 4. Cumulative urinary activity excretion for patients 1, 3, 5, and 9. Data are decay-corrected and normalized to IC in intraperitoneal fluid. hpi = hours post infusion.

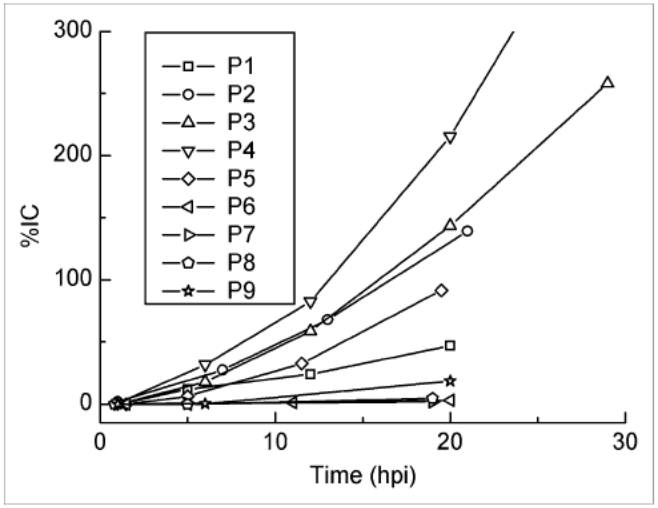

FIGURE 6. Thyroid ^{211}At activity concentration in patients 1–9 calculated from AP scans. Patient 4 had 872% IC at 48 h (cut from graph). Patients 6–8 were blocked with potassium perchlorate, patient 9 with potassium iodide. Data are decay-corrected and normalized to IC in intraperitoneal fluid. AP = anteroposterior; hpi = hours post infusion.

- Bone marrow dosimetry was based on serum activity concentration data.

TABLE 1. Treatment Specifications and Absorbed Doses to Organs at Risk

Patient no.	IC (MBq/L)	Administered volume (L)	Absorbed dose (Gy)			
			Bone marrow	Thyroid	Peritoneal lining	Urinary bladder epithelium
1	22.4	1.5	0.0031	0.20	0.28	0.013
2	24.2	2.0	0.0020	0.59	0.31	—
3	20.1	2.0	0.0039	0.52	0.29	0.016
4	21.1	2.0	0.0032	0.80	0.33	—
5	46.2	2.0	0.0085	0.82	0.66	0.044
6	47.4	2.18	0.0094	0.02	0.69	—
7	101	1.18	0.0091	0.03	1.59	—
8	72.6	1.14	0.0107	0.07	0.91	—
9	53.4	1.21	0.0055	0.18	0.77	0.030

Advancing Alpha Particle Therapy using Nuclear Nanotechnologies

Theranostics

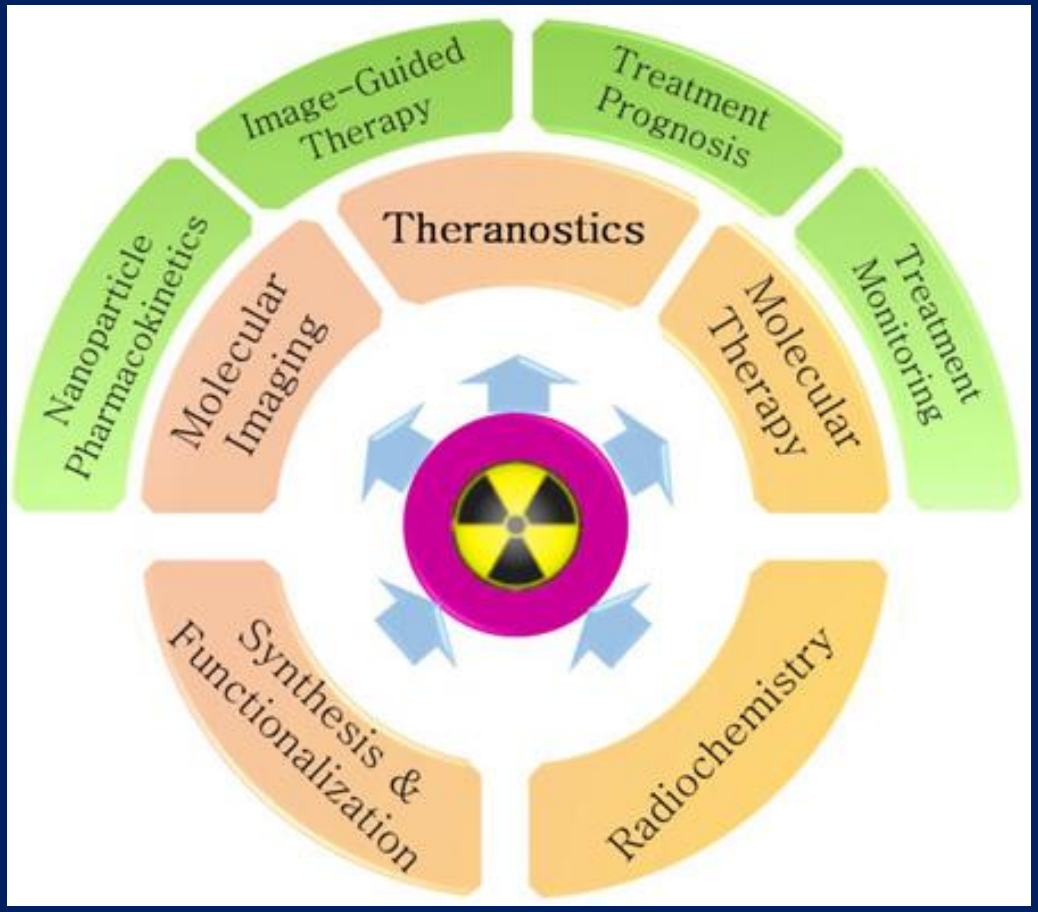

S. Goel, C. G. England, F. Chen, and W. Cai, "Positron emission tomography and nanotechnology: A dynamic duo for cancer theranostics.," *Adv Drug Deliv Rev*, vol. 113, pp. 157–176, Apr. 2017.

Five Major Strategies For Radiolabeling Nanomaterials

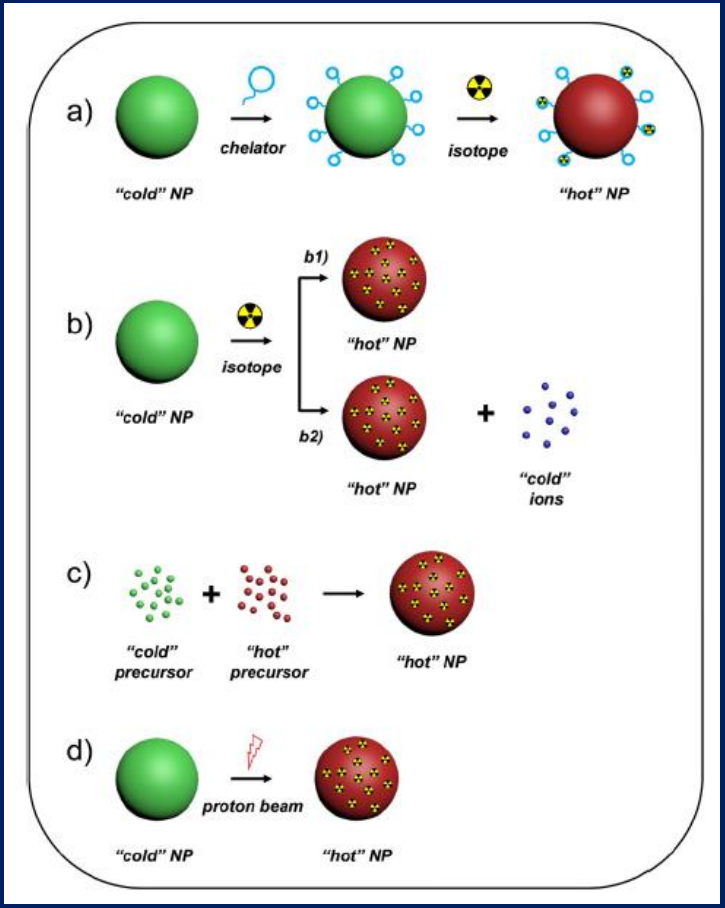

S. Goel, C. G. England, F. Chen, and W. Cai, "Positron emission tomography and nanotechnology: A dynamic duo for cancer theranostics.," *Adv Drug Deliv Rev*, vol. 113, pp. 157–176, Apr. 2017.

Encapsulation of α-Particle–Emitting $^{225}Ac^{3+}$ Ions Within Carbon Nanotubes

Michael L. Matson[1], Carlos H. Villa[2], Jeyarama S. Ananta[1,3], Justin J. Law[1], David A. Scheinberg[2], and Lon J. Wilson[1]

[1]Department of Chemistry, and the Smalley Institute for Nanoscale Science and Technology, Rice University, Houston, Texas; [2]Molecular Pharmacology and Chemistry Program, Memorial Sloan Kettering Cancer Center, and Weill Cornell Medical College, New York, New York; and [3]Molecular Imaging Program at Stanford University, Department of Radiology, Stanford University, Stanford, California

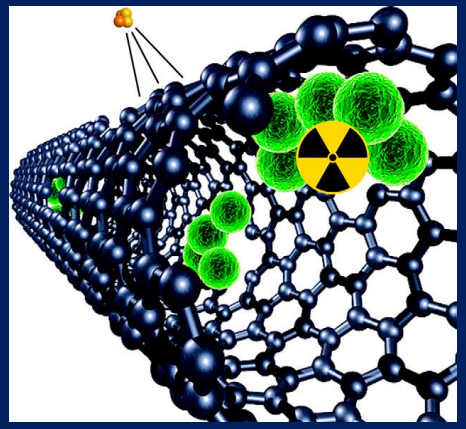

M. L. Matson, C. H. Villa, J. S. Ananta, J. J. Law, D. A. Scheinberg, and L. J. Wilson, "Encapsulation of α-Particle-Emitting 225Ac3+ Ions Within Carbon Nanotubes.," *J Nucl Med*, vol. 56, no. 6, pp. 897–900, Jun. 2015.

^{64}Cu-AuNPs

Representative PET/CT images at 1 h, 24 h, 48 h post-injection of alloyed ^{64}CuAuNPs and 18F-FDG at 1 h in EMT-6 tumor-bearing mice (green arrow T: tumor).

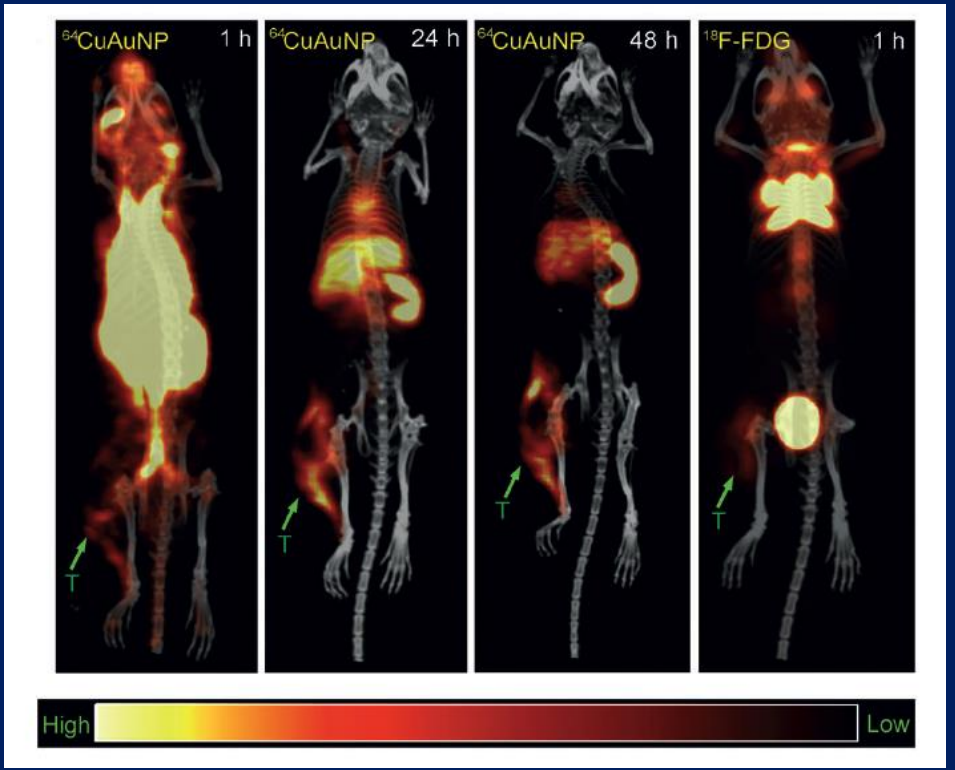

Y. Zhao, D. Sultan, L. Detering, S. Cho, G. Sun, R. Pierce, K. L. Wooley, and Y. Liu, "Copper-64-alloyed gold nanoparticles for cancer imaging: improved radiolabel stability and diagnostic accuracy.," *Angew Chem Int Ed Engl*, vol. 53, no. 1, pp. 156–159, Jan. 2014.

Applied Radiation and Isotopes 131 (2018) 49–57

Contents lists available at ScienceDirect

Applied Radiation and Isotopes

journal homepage: www.elsevier.com/locate/apradiso

Rapid synthesis of ^{125}I integrated gold nanoparticles for use in combined neoplasm imaging and targeted radionuclide therapy

Ryan Clanton[a,c,*], Arnulfo Gonzalez[a], Sriram Shankar[a], Gamal Akabani[a,b,c]

[a] Department of Nuclear Engineering, Texas A&M University, College Station, TX 77843, United States
[b] Department of Veterinary Integrative Biosciences, Texas A&M University, College Station, TX 77843, United States
[c] Texas A&M Institute for Preclinical Studies, Texas A&M University, College Station, TX 77843, United States

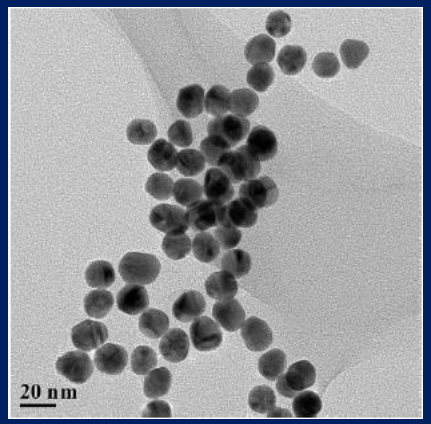

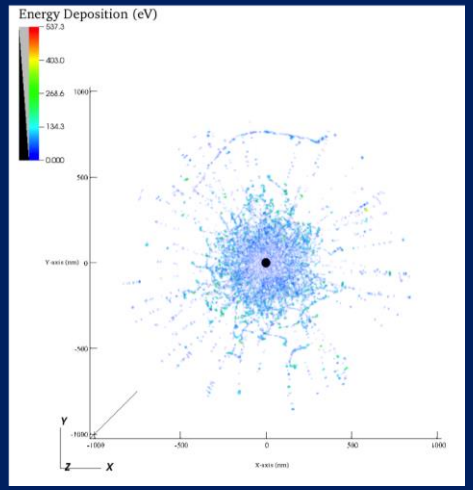

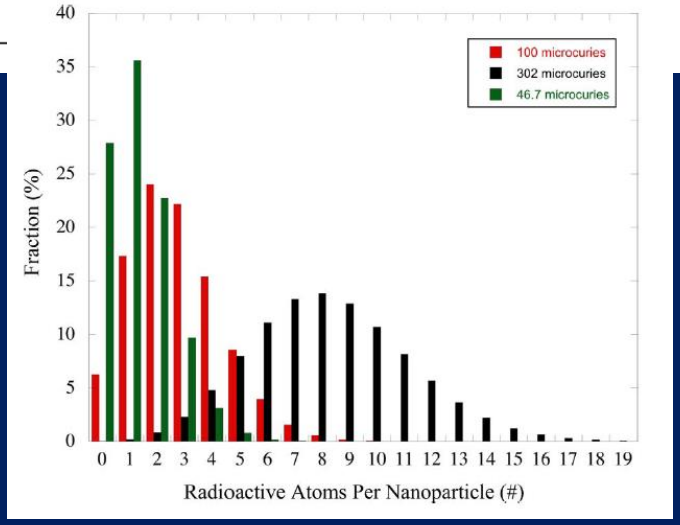

$$P(x \cap d;\, t) = \frac{e^{-\mu}\mu^{x}}{d!(x-d)!}(1-e^{-\lambda t})^{d}(e^{-\lambda t})^{x-d}.$$

Binary radioactive NPs

- We desire the combination of a PET or SPECT imaging radionuclide and an alpha particle or Auger emitting radionuclide.

Examples

- Alpha/PET-AuNPs
- Auger/PET-AuNPs
- Beta/PET-AuNPs

Conclusions

Conclusions

- Dosimetry is a continuum
  - From In vitro studies and models
  - To high fidelity animal models of human cancer
  - To clinical trials
- Dosimetry of alpha particle radiotherapeutics needs to consider and incorporate the spatiotemporal pathophysiology and morphology of the tumor tissues at the same scale of the range of alpha particles in tissues to assess its benefits and limitations